UNIVERSIDAD DE CONCEPCIÓN
FACULTAD DE CIENCIAS FÍSICAS Y MATEMÁTICAS

QUANTUM CORRECTIONS TO NEAR EXTREMAL BLACK HOLE ENTROPY AND HIGHER CURVATURE TERMS

Por: Jorge Urbina Cabrera

Tesis presentada a la Facultad de Ciencias Físicas y Matemáticas de la Universidad de Concepción para optar al grado académico de Magíster en Ciencias con Mención en Física

Mayo 2026
Concepción, Chile

Profesor guía:
Dr. Julio Oliva Zapata

Profesor Co-guía:
Dr. Marcelo Oyarzo Catalán

A mis padres y hermana.

AGRADECIMIENTOS

Quiero agradecer a todas las personas que me han acompañado y sostenido a lo largo de este camino. Este trabajo marca el cierre de una etapa importante, pero también es el resultado de muchos años de apoyo, compañía y aprendizaje compartido.

A mi familia: mis padres, Jorge y Sandra, y mi hermana Sylvana. Su apoyo incondicional ha sido fundamental en todos los ámbitos de mi vida y una de las razones que me ha permitido persistir en cada etapa de este recorrido. Gracias por estar siempre ahí, por la confianza, el cariño y el respaldo constante. Estaré siempre profundamente agradecido por todo lo que han hecho por mí.

El camino del aprendizaje habría sido mucho más difícil sin mis profesores. Quiero agradecer especialmente a mi director de tesis, el Dr. Julio Oliva, y a mi co-director, el Dr. Marcelo Oyarzo. Estos últimos meses habrían sido significativamente más difíciles sin su apoyo permanente, su disposición y su guía. Conocer a Marcelo durante esta etapa ha sido una grata sorpresa: además de haber sido un co-guía atento y generoso, he podido conocer a una gran persona. Agradezco también de manera especial al Dr. Andrés Anabalón, siempre dispuesto a aclarar una duda, y al Dr. Guillermo Rubilar, porque junto a él fueron los primeros profesores en mostrarme la belleza de la Relatividad General. Del mismo modo, debo una parte importante de mi entusiasmo por la teoría al Dr. Juan Crisóstomo, quien siempre alimentó mi deseo de seguir aprendiendo y de cuestionar las cosas. Gracias sinceras a todos ustedes.

En una carrera tan absorbente como la científica, compartir con los amigos ha sido siempre un apoyo fundamental. De distintas maneras, todos han sido parte importante de este proceso. Con Gabriel he compartido derrotas y victorias a lo largo de estos años; tanto en lo académico como en lo personal, muchas veces nos ha tocado salir adelante siendo uno el apoyo del otro. A Alfredo, amigo de gran parte de mi vida, le agradezco su empatía, su forma apañadora de estar presente y el haberme ayudado a mirar y comprender otros aspectos de la vida; en el camino hemos aprendido mucho el uno del otro. También quiero agradecer a sus padres, por recibirme siempre con cariño en su casa y hacerme sentir parte

de ella. Al Seba, por sacarme siempre una carcajada y por estar presente con apoyo y buena energía cuando ha hecho falta. Y a Cristóbal, por las incesantes y variadas conversaciones sobre todo tipo de temas, que tantas veces me han ayudado a redireccionar y replantear mis pensamientos.

Mirando hacia atrás, me doy cuenta de que este recorrido no habría sido el mismo sin cada una de estas personas. Más allá de lo académico, lo que permanece son los vínculos, las conversaciones, el apoyo en los momentos difíciles y todo lo compartido durante estos años. Este cierre también les pertenece.

Resumen

Esta tesis investiga las correcciones cuánticas a un loop a la entropía de agujeros negros cercanos a la extremalidad en gravedad de Einstein-Gauss-Bonnet (EGB) acoplada a un campo de Maxwell en cinco dimensiones. Se estudia una solución puramente eléctrica que admite un límite extremal. En este límite, la termodinámica clásica predice una gran degeneración del estado fundamental. El análisis se centra en el régimen cercano a la extremalidad, donde al disminuir la temperatura la emisión de un cuanto de Hawking puede producir variaciones apreciables en el estado térmico, lo que plantea interrogantes conceptuales sobre la validez de la descripción semiclásica.

Para abordar estos problemas, se emplea el formalismo de la integral de camino euclidiana y se calcula la función de partición en la aproximación semiclásica. El análisis se realiza expandiendo la acción hasta segundo orden en la métrica y el campo de gauge alrededor de la geometría cerca del horizonte, la cual desarrolla una estructura $\mathrm{AdS}_2 \times S^3$ en el límite extremal. En este marco, las correcciones cuánticas quedan codificadas en el espectro de un operador generalizado de Lichnerowicz que gobierna las fluctuaciones de la métrica y del campo de gauge.

Una característica clave de este operador es la presencia de modos cero en el límite extremal, los cuales conducen a divergencias en la función de partición a un loop. Se muestra que, en el régimen cercano a la extremalidad, estos modos dejan de ser modos cero y adquieren autovalores proporcionales a la temperatura, dando lugar a correcciones logarítmicas a la entropía.

Los resultados proporcionan una realización concreta de cómo los efectos cuánticos modifican la descripción semiclásica de agujeros negros en teorías de gravedad con curvatura superior, y develan la estructura de la densidad de estados en el régimen cercano a la extremalidad.

Palabras clave: Agujeros negros, agujeros negros cercanos a la extremalidad, gravedad de Einstein-Gauss-Bonnet, correcciones cuánticas, efectos a un loop, integral de camino, geometría cerca del horizonte, determinantes funcionales, modos cero, entropía de agujeros negros

Abstract

This thesis investigates the one-loop quantum corrections to the entropy of near-extremal black holes in five-dimensional Einstein-Gauss-Bonnet (EGB) gravity coupled to a Maxwell field. A purely electric solution admitting an extremal limit is considered. In this limit, classical thermodynamics predicts a large ground-state degeneracy. The analysis focuses on the near-extremal regime, where, as the temperature decreases, the emission of a Hawking quantum can induce appreciable changes in the thermal state, raising conceptual questions about the validity of the semiclassical description

To address these issues, the Euclidean path integral formalism is employed to compute the partition function in the semiclassical approximation. The analysis is performed by expanding the action to quadratic order in the metric and the gauge field around the near-horizon geometry, which develops an $\mathrm{AdS}_2 \times S^3$ structure in the extremnal limit. In this framework, quantum corrections are encoded in the spectrum of a generalized Lichnerowicz operator governing fluctuations of the metric and the gauge field.

A key feature of this operator is the presence of zero modes in the extremal limit, which lead to divergences in the one loop partition function. It is shown that, in the near-extremal regime, these modes are lifted and acquire eigenvalues proportional to the temperature, giving rise to logarithmic corrections to the entropy.

The results provide a concrete realization of how quantum effects modify the semiclassical description of black holes in higher-curvature gravity, and shed light on the structure of the near-extremal density of states.

Keywords: black holes, near-extremal black holes, Einstein Gauss Bonnet gravity, quantum corrections, one-loop effects, path integral, near-horizon geometry, functional determinants, zero modes, black hole entropy

Contents

List of Figures

Chapter 1

Introduction

Modern physics rests on two extraordinarily successful conceptual pillars: General Relativity and quantum mechanics. General Relativity describes gravity as a manifestation of the geometry of spacetime, providing a classical theory whose validity has been confirmed across a wide range of scales, from tests in the solar system to highly energetic phenomena from mergers of compact objects [1]. On the other hand, quantum mechanics, consistently formulated through quantum field theory, constitutes the fundamental framework for describing matter and non-gravitational interactions, as for example in the Standard Model of particle physics, whose predictive accuracy is unprecedented.

Despite these achievements, both theories rely on conceptual principles that are not easily compatible. While General Relativity treats spacetime as a dynamical object whose geometry evolves in response to matter content, quantum mechanics is typically formulated on a fixed background on which quantum fields propagate. This tension becomes unavoidable in regimes where both gravitational and quantum effects are simultaneously relevant, such as near singularities or in the early stages of the universe. The absence of a fully consistent theory of quantum gravity therefore reflects a fundamental limitation in our current understanding of nature.

In this context, black holes emerge as privileged systems for exploring the intersection between these two frameworks. Originally conceived as classical solutions to Einstein's equations, black holes represent regions of spacetime bounded by an event horizon, beyond which no signals can be sent to infinity.

However, their relevance extends beyond the purely classical domain.

A decisive breakthrough occurred in the 1970s, when Jacob Bekenstein and Stephen Hawking showed that black holes admit a thermodynamic description [2, 3]. In particular, it was established that a black hole can be assigned an entropy and a temperature given by

$$S_{\mathrm{BH}} = \frac{A}{4G\hbar}, \qquad T_{\mathrm{H}} = \frac{\kappa}{2\pi}, \tag{1.0.1}$$

where A is the horizon area and κ its surface gravity. This result introduces a profound connection between gravity, quantum mechanics, and thermodynamics. Indeed, Hawking temperature arises from considering quantum fields propagating on a classical gravitational background, implying that black holes emit thermal radiation.

Conceptual Tensions and Motivation

The existence of Hawking radiation gives rise to a number of conceptual problems. In particular, if the evolution of a black hole leads to the emission of thermal radiation and eventually to its complete evaporation, it would appear that information about the initial state is lost, in apparent contradiction with the unitarity of quantum mechanics. This tension constitutes the core of the information paradox.

From a statistical perspective, the very notion of entropy raises a further fundamental question: if entropy measures the number of microstates accessible to a macroscopic system, what is the nature of the microstates underlying a black hole?

Large ground state degeneracy of extremal black holes

Beyond the question of the microscopic origin of the Bekenstein-Hawking entropy, there exist regimes in which even the validity of the formula itself becomes questionable. One such regime is provided by a particular class of black holes, known as extremal black holes.

In general, a black hole solution is characterized by a set of conserved charges, such as its mass M, angular momentum J, and electric charge Q. For fixed values of these charges, the existence of an event horizon imposes a lower bound on the mass, which can be schematically written as $M \geq M_{\text{ext}}(Q, J)$. The extremal limit is defined by the saturation of this bound, $M = M_{\text{ext}}$.

In this limit, the structure of the spacetime undergoes a qualitative change: the inner and outer horizons coincide, leading to a degenerate horizon. As a consequence, the surface gravity vanishes and therefore the Hawking temperature is zero, while the horizon area remains finite.

On the one hand, the third law of thermodynamics in its Nernst formulation states that the entropy of a thermodynamic system should vanish as the temperature approaches zero. However, extremal black holes have vanishing Hawking temperature while possessing non-zero entropy. For example, in four-dimensional asymptotically flat Einstein-Maxwell theory a charged rotating black hole with electric charge Q and angular momentum J has extremal entropy given by

$$S_{\text{ext}} = \frac{A_{\text{ext}}}{4G} = \pi\sqrt{Q^4 + 4J^2}. \tag{1.0.2}$$

For macroscopic black holes (not necessarily astrophysical), $Q \gg 1$ and $J \gg 1$, implying

$$S_{\text{ext}} \gg 1. \tag{1.0.3}$$

This suggests a very large ground state degeneracy. Equivalently, since $S_{\text{ext}} \sim A_{\text{ext}}/\ell_p^2$, the semiclassical regime corresponds to horizon areas much larger than the Planck area.

Such large degeneracies are typically realized in systems that are either effectively free or possess a large number of weakly interacting degrees of freedom. A standard example is provided by Landau levels: for a charged particle in a uniform magnetic field, each energy level contains a macroscopic degeneracy whose degeneracy is proportional to the area of the sample. Another example is an antiferromagnetic spin system on a triangular lattice, where geometric frustration prevents all pairwise interactions from being simultaneously minimized, producing a large number of nearly degenerate low-energy configurations.

In contrast, the microscopic quantum dynamics relevant for black holes is generally expected to be strongly coupled. This expectation is supported, for example, by holography, where black holes are related to strongly interacting conformal field theories [4, 5]. From this perspective, extremal black holes appear to lie well outside the regime in which the conventional counterexamples to the Nernst formulation of the third law usually arise.

Hawking raditation for near-extremal black holes

A different issue concerning the validity of the Bekenstein-Hawking entropy arises for near-extremal black holes and was emphasized by [6–8]. The usual thermodynamic or statistical description of black holes relies on the assumption that the emission of a single Hawking quantum does not significantly change the temperature. However, the temperature of a black hole depends on its energy E, charge Q, and angular momentum J, i.e., $T = T(E, Q, J)$. When the black hole emits a quantum of radiation, it loses an amount of energy δE, leading to a change in temperature δT.

Expanding the temperature around E, one finds

$$T(E + \delta E) = T(E) + \left.\frac{\partial T}{\partial E}\right|_{Q,J} \delta E + \mathcal{O}((\delta E)^2), \tag{1.0.4}$$

therefore, to first order in δE,

$$\delta T = \left.\frac{\partial T}{\partial E}\right|_{Q,J} \delta E. \tag{1.0.5}$$

Since the emitted radiation carries away energy from the black hole, the corresponding variation of its energy is negative, $\delta E < 0$. Moreover, the typical energy of a Hawking quanta, because of Wien's law, is of the order of the temperature, $\delta E \sim -T$. Therefore, the relative change in temperature is

$$\frac{\delta T}{T} = \left.\frac{\partial T}{\partial E}\right|_{Q,J}. \tag{1.0.6}$$

A broad variety of near-extremal black holes exhibit this low-temperature structure, including the Reissner-Nordström, Kerr, and Kerr-Newman families, as well as charged black holes in asymptotically AdS spacetimes. For this broad class of solutions, and at fixed Q and J, the energy above extremality and the entropy admit expansions of the form

$$E \equiv M - M_{\text{ext}} = \frac{T^2}{E_b} + \mathcal{O}(T^3), \tag{1.0.7}$$

$$S = S_{\text{ext}} + c_b\, T + \mathcal{O}(T^2), \tag{1.0.8}$$

where E_b defines the coefficient of the quadratic term in the expansion of the mass, and depends on the conserved charges that are considering to be fixed, while c_b is a solution-dependent constant which is generally proportional to E_b^{-1}, although it does not necessarily coincide with it exactly. While the precise coefficients depend on the particular black hole solution, the leading scaling behaviour (1.0.7) and (1.0.8) appear to be a general feature for extremal black holes in the near-extremal regime.

Therefore, for this class of near-extremal black holes, combining (1.0.6) with (1.0.7) gives

$$\frac{\delta T}{T} = \frac{1}{2}\frac{E_b}{T}. \tag{1.0.9}$$

Thus,

$$\frac{\delta T}{T} \gg 1 \tag{1.0.10}$$

when $T \lesssim E_b$. This indicates that, in the near-extremal regime, the emission of a single quantum induces an $\mathcal{O}(1)$ change in the temperature, indicating a breakdown of the standard thermodynamic description even before extremality is reached. The structure described above has important implications for the spectrum of excitations near extremality. In particular, the combination of a large ground state degeneracy and a finite energy gap leads to a highly constrained set of accessible states at low energies. This behavior is schematically illustrated in Fig. 1.0.1.

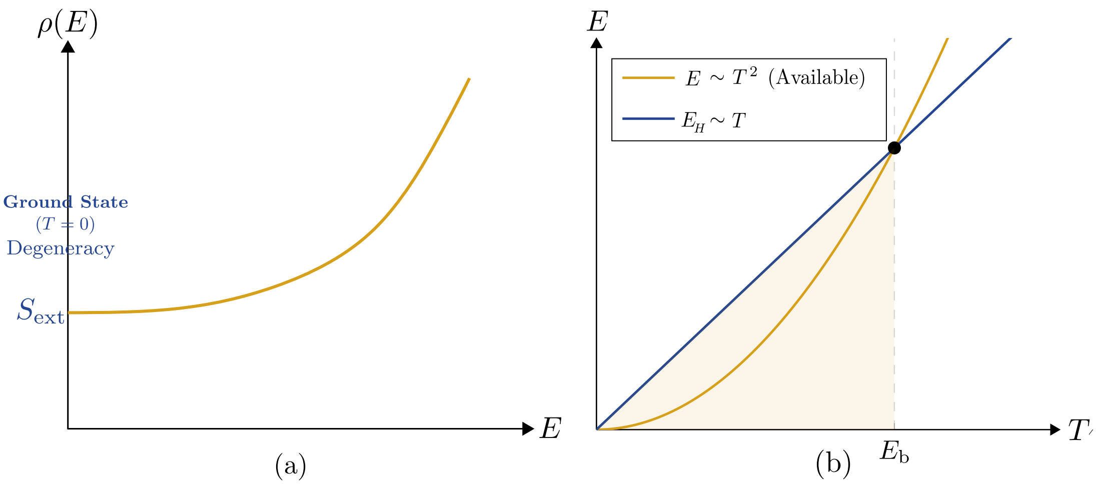

Figure 1.0.1: (a) Qualitative behavior of the density of microstates $\rho(E)$ as a function of the energy E above extremality. The extremal configuration at $E = 0$ exhibits a macroscopic entropy $S_{\text{ext}} \gg 1$, corresponding to a highly degenerate ground state. (b) The curve in gold represents the energy available of a black hole above extremality, $E = M - M_{\text{ext}}$, as a function of its temperature T, while the blue curve represents the energy of a Hawking quantum, E_H, as a function of T. In the near-extremal regime, the energy scales as $E \sim T^2/E_b$, whereas the typical energy of Hawking quanta is $E_H \sim T$. When $T \lesssim E_b$, the black hole does not have enough available energy to emit a Hawking quantum. This structure implies that, at sufficiently low temperatures, the available energy above extremality is insufficient to excite higher states, which plays a central role in the breakdown of the standard thermodynamic description of near-extremal black holes.

How can these issues be reconciled? In 2020, Maldacena and collaborators [9] proposed the so-called *central dogma*, which states that, for an external observer, a black hole can be described as an ordinary quantum system with a finite number of degrees of freedom proportional to the horizon area, evolving unitarily. This viewpoint encapsulates the idea that, despite the semiclassical description, the full dynamics of black holes should be compatible with standard quantum mechanics.

One logical possibility would be to abandon this principle and conclude that black holes are not ordinary quantum systems. However, there is no concrete evidence supporting this possibility. On the contrary, the central dogma is supported by several independent lines of evidence within string theory: (i) holography via AdS/CFT, which ensures unitarity; (ii) microscopic derivations of black hole entropy matching the Bekenstein-Hawking formula [10]; and (iii) dynamical studies of thermalization and chaos in strongly coupled quantum systems. No controlled counterexamples are known.

The alternative is to accept that quantum gravitational effects become relevant in the near-extremal regime, even at low temperatures. A potential objection to this viewpoint is that the curvature near the horizon of an extremal black hole can be made arbitrarily small by taking the conserved charges to be large. This might suggest that quantum gravity effects should be negligible, since they are commonly expected to become important only in regions of large curvature, such as spacetime singularities.

However, this reasoning is not conclusive. The smallness of curvature invariants does not, by itself, guarantee the suppression of quantum effects. Whether quantum corrections are relevant is a subtle question that must be addressed through explicit calculations, rather than inferred solely from dimensional arguments.

Therefore, if one insists on the validity of the central dogma, the question becomes unavoidable: what is the origin of quantum effects capable of modifying the semiclassical result $S_{\text{ext}} \gg 1$?

This question suggests that the Bekenstein-Hawking entropy should admit a microscopic interpretation within a theory of quantum gravity. In the absence of a complete formulation of such a theory, however, one must proceed indirectly.

Rather than attempting a first-principles derivation of the microscopic degrees of freedom, a natural strategy is to study how quantum effects modify the semiclassical entropy formula.

The appropriate framework for this problem is the Euclidean gravitational path integral. In the Euclidean formulation, the gravitational partition function is formally defined by

$$Z = \int \mathcal{D}\Phi e^{-I[\Phi]}, \tag{1.0.11}$$

where Φ collectively denotes the dynamical fields and $I[\Phi]$ is the Euclidean action.

When the Euclidean time direction is periodic, the partition function admits a thermodynamic interpretation: the free energy, entropy, and other thermal quantities can be extracted from $\log Z$. From this perspective, the thermodynamic properties of black holes are directly determined by the underlying gravitational action.

This simple observation already suggests the relevance of higher-curvature interactions. If the Einstein-Hilbert action provides only the leading contribution to the low-energy effective description of gravity, then modifying the action necessarily modifies the partition function and therefore the quantum corrections to black hole thermodynamics.

In the semiclassical approximation, the path integral is dominated by saddle points of the classical action, while the leading quantum contribution arises from fluctuations around the corresponding background. Expanding the fields around a classical solution, the one-loop correction is governed by the quadratic fluctuation operator. Therefore, the problem of computing quantum corrections to black hole entropy reduces to a spectral problem: one must determine how the eigenvalues of the fluctuation operator behave in the near-horizon geometry of the relevant black hole background.

This observation becomes particularly significant in the near-extremal regime. As will be discussed below, extremal black holes develop a decoupled near-horizon region containing an AdS_2 factor. In such geometries, the fluctuation operator may develop zero modes. Their presence reflects an enhanced degeneracy of the semiclassical background and leads to infrared singularities in the one-loop partition function. At small but finite temperature, these zero modes are expected to be lifted, generating small eigenvalues that can produce logarithmic contributions to the entropy.

A natural question then arises. If the gravitational dynamics is modified by higher-curvature interactions, how are the spectrum of fluctuations and the resulting quantum corrections affected?

From the viewpoint of effective field theory, the Einstein-Hilbert action should be regarded as the leading term in a derivative expansion valid below the ultraviolet completion [11]. At low energies, the effective action is therefore expected to contain higher-order curvature invariants of the schematic form

$$S_{\text{eff}} = \frac{1}{16\pi G} \int d^d x \sqrt{-g} \left(R + \alpha_1 R^2 + \alpha_2 R_{\mu\nu} R^{\mu\nu} + \cdots \right). \tag{1.0.12}$$

Once such terms are included, the quadratic fluctuation operator around a non-trivial background is no longer the one obtained in pure Einstein gravity, but rather a deformation of it. Consequently, the one-loop partition function, and therefore the logarithmic corrections to black hole entropy, can acquire a non-trivial dependence on the new couplings appearing in the effective theory.

Within this broader class of theories, Einstein-Gauss-Bonnet gravity occupies a distinguished position. It corresponds to the first non-trivial member of Lovelock's hierarchy of higher-curvature theories. More precisely, it is the most general extension of Einstein gravity whose field equations remain second order in the metric [12]. In four spacetime dimensions, the Gauss-Bonnet combination is purely topological and does not modify the local dynamics. By contrast, in five or more dimensions it contributes non-trivially to the equations of motion, providing one of the simplest settings in which higher-curvature effects become dynamically relevant.

The particular combination of quadratic curvature invariants defining the Gauss-Bonnet term also avoids the appearance of additional ghost-like degrees of freedom [13]. Moreover, such terms arise naturally as leading α' corrections in string theory, in particular in heterotic string theory up to field redefinitions [14, 15], providing an independent physical motivation for their study.

Beyond this general theoretical relevance, the Einstein-Gauss-Bonnet theory coupled to a Maxwell field provides a particularly useful setting for the present problem. In contrast with Einstein gravity, exact rotating black hole solutions at finite Gauss-Bonnet coupling are not known in closed analytic form, with existing results being mostly numerical or perturbative [16]. Charged static solutions, however, are available analytically and possess a well-defined extremal branch. This makes the Einstein-Maxwell-Gauss-Bonnet system especially suitable for investigating near-extremal quantum effects.

In five dimensions, near-extremal black holes develop a near-horizon geometry containing an $AdS_2 \times S^3$ throat whose geometric scales depend explicitly on the Gauss-Bonnet coupling.. This makes it possible to formulate sharply the question that motivates this work: how does the higher-curvature coupling modify the spectrum of quantum fluctuations around the near-horizon geometry, and what is its effect on the logarithmic corrections to the entropy?

The question of logarithmic quantum corrections to black hole entropy has been studied in several related settings over the past decades. Early analyses within quantum field theory in curved spacetime showed that logarithmic corrections emerge from the evaluation of functional determinants using heat-kernel techniques, and are closely related to conformal anomalies [17, 18].

Later, in theories with extended supersymmetry, the quantum entropy function formalism developed by Ashoke Sen provided a systematic framework for computing these contributions in extremal black holes. In this approach, the logarithmic coefficient is determined by the spectrum of fluctuations around the near-horizon geometry [19, 20]. In supersymmetric settings, non-trivial cancellations between bosonic and fermionic modes can strongly constrain the structure of the corrections.

Beyond the supersymmetric regime, subsequent studies extended these analyses to non-BPS black holes, rotating configurations, and near-extremal geometries, where protected cancellations are generally absent and the logarithmic coefficient acquires a richer dependence on field content and boundary conditions [21, 22]. In parallel, holographic approaches have reinterpreted these effects in terms of dual conformal field theories, further clarifying the relation between gravitational thermodynamics and microscopic degrees of freedom [23].

These developments indicate that the study of quantum corrections to black hole entropy should not be regarded merely as a technical refinement. Since different proposals for quantum gravity may agree on the leading semiclassical contribution while differing in subleading terms, a detailed analysis of logarithmic corrections provides a sensitive probe of the microscopic structure of black holes.

The present work addresses this problem in the context of higher-curvature gravity, focusing on the near-extremal regime of charged black holes in Einstein-Gauss-Bonnet theory.

Motivated by these considerations, the main objective of this thesis is to determine how the higher-curvature coupling modifies the spectrum of fluctuations around the near-horizon geometry and how this dependence is reflected in the one-loop partition function.

More specifically, we study five-dimensional charged black hole solutions admitting an extremal branch. Within this setting, the problem reduces to the analysis of the generalized fluctuation operator governing metric and gauge-field perturbations, with particular emphasis on the role of zero modes and their lifting at small but finite temperature.

The structure of this thesis is as follows.

In Chapter 2, we introduce the path integral formulation of the partition function and its semiclassical approximation. In this context, we explain how quantum corrections arise from fluctuations around classical solutions and how they are encoded in functional determinants. As a preliminary step, we analyze the quantum harmonic oscillator as a solvable example, illustrating these ideas in a controlled setting.

In Chapter 3, we present the Einstein-Gauss-Bonnet theory coupled to a Maxwell field and review the corresponding charged black hole solutions. We discuss their thermodynamic properties, with particular emphasis on the extremal and near-extremal regimes, where a finite mass gap and a large ground-state degeneracy emerge.

In Chapter 4, we focus on the near-horizon geometry of near-extremal black holes. We show how, in the zero-temperature limit, the geometry develops an $\mathrm{AdS}_2 \times S^3$ throat that effectively decouples from the asymptotic region, providing the natural background for the quantum analysis.

In Chapter 5, we construct the quadratic action for fluctuations around this near-horizon background and derive the differential operator governing the dynamics of perturbations. We analyze its spectrum, paying special attention to the role of zero modes and their lifting in the near-extremal regime.

Finally, using these results, we evaluate the one-loop partition function and discuss the resulting logarithmic corrections to black hole entropy, with particular emphasis on their implications for the near-extremal density of states. We conclude with a summary of the main results and a discussion of possible directions for future research.

Chapter 2

Partition Function

2.1 Partition Function and the Semiclassical Approximation

This chapter introduces the main tool that underlies the rest of this thesis: the Euclidean partition function. As emphasized in the Introduction, our goal is to study quantum corrections to near-extremal black hole thermodynamics. In this setting, the partition function is the natural object because it encodes both the thermodynamic information of the classical background and the quantum fluctuations around it.

In gravitational systems, the Euclidean partition function is formally defined by

$$Z = \int \mathcal{D}\phi \; e^{-I_E[\phi]}, \tag{2.1.1}$$

where ϕ collectively denotes the dynamical fields and I_E is the Euclidean action. The functional integral is taken over field configurations satisfying prescribed Euclidean boundary conditions. In the semiclassical regime, the dominant contributions arise from stationary points of the Euclidean action.

When the Euclidean time direction is periodic with period β, the contribution of a given saddle admits a thermodynamic interpretation. The period β is identified with the inverse temperature,

$$\beta = \frac{1}{T}, \tag{2.1.2}$$

and thermodynamic quantities are extracted from the $\log Z$. In particular, the free energy and entropy are given by

$$F = -\frac{1}{\beta}\log Z, \qquad M = -\frac{\partial}{\partial\beta}\log Z, \qquad S = \left(1 - \beta\frac{\partial}{\partial\beta}\right)\log Z. \tag{2.1.3}$$

For the problem studied here, quantum corrections to black hole entropy arise from the quantum contribution to this quantity [24].

The difficulty, of course, is that this path integral is defined over an infinite-dimensional space of field configurations and in general is not exactly computable. The appropriate approximation scheme is therefore the saddle-point, or semiclassical, expansion around a stationary point of the Euclidean action.

The dominant configurations are therefore classical saddles $\bar{\phi}$ satisfying

$$\left.\frac{\delta I_E}{\delta\phi}\right|_{\bar{\phi}} = 0. \tag{2.1.4}$$

To extract quantum effects, one writes

$$\phi = \bar{\phi} + \eta, \tag{2.1.5}$$

and expands the action as a power series in η,

$$I_E[\phi] = I_E[\bar{\phi}] + I^{(1)}[\eta] + I^{(2)}[\eta] + \mathcal{O}(\eta^3). \tag{2.1.6}$$

The linear term vanishes on-shell, so the leading quantum contribution is governed by the quadratic term.

If the quadratic action takes the form

$$I^{(2)}[\eta] = \frac{1}{2}\int d^d x\, \eta\, \mathcal{O}\, \eta, \tag{2.1.7}$$

where d denotes the spacetime dimension and $\mathcal{O}$ is the differential operator determined by the background, then the path integral becomes,

$$Z \approx e^{-I_E[\bar{\phi}]}\int \mathcal{D}\eta\, e^{-I^{(2)}[\eta]}. \tag{2.1.8}$$

The expression above is a Gaussian functional integral, whose result is determined by the functional determinant of the operator $\mathcal{O}$ as

$$Z \approx e^{-I_E[\bar{\phi}]} \, (\det \mathcal{O})^{-1/2}. \tag{2.1.9}$$

Therefore,

$$\log Z = -I_E[\bar{\phi}] - \frac{1}{2} \log \det \mathcal{O}, \tag{2.1.10}$$

which already exhibits the structure that will be central in what follows: a classical contribution from the on-shell action and a one-loop correction encoded in the determinant of the fluctuation operator.

For the purposes of this thesis, this framework isolates the ingredients that must later be identified in the black holes problem: a relevant classical saddle, the quadratic fluctuation operator around it, and the associated zero modes. The near-horizon region of the corresponding extremal solution generally takes the form

$$AdS_2 \times \mathcal{M}, \tag{2.1.11}$$

with $\mathcal{M}$ compact. For extremal rotating black holes with a $U(1)$ fiber, this factorization provides the geometric setting in which the one-loop partition function and the associated logarithmic corrections to entropy will be studied [25].

The logic of the semiclassical expansion can also be illustrated in a simpler setting. Consider the ordinary integral

$$Z = \int dx \, e^{-\frac{1}{\hbar} S(x)}, \tag{2.1.12}$$

whose dominant contribution in the limit $\hbar \to 0$ comes from the extrema of $S(x)$. This finite-dimensional example is included only as a familiar analogue of the saddle-point approximation and should be understood merely as an illustration of the general structure described above.

Before turning to the gravitational case, however, it is useful to study a simpler example in which the same logic can be followed explicitly. The harmonic oscillator can be solved both from the canonical definition of the partition function and from the Euclidean path integral. Since its action is already quadratic, the Gaussian path integral gives the exact result rather than only the first one-loop correction. Nevertheless, this example remains an ideal prototype for understanding how functional determinants, normalization factors, and zero modes arise in the semiclassical treatment that will later be applied to black hole backgrounds.

2.2 The Quantum Harmonic Oscillator

The energy levels of a harmonic oscillator with frequency ω are given by:

$$E_n = \hbar\omega\left(n + \frac{1}{2}\right), \quad n = 0, 1, 2, \dots \tag{2.2.1}$$

By expressing the partition function Z as a sum over all possible states using the eigenvalues from Eq. (2.2.1), we obtain:

$$\begin{aligned} Z = \sum_n e^{-\beta E_n} &= \sum_{n=0}^{\infty} e^{-\beta\hbar\omega\left(n+\frac{1}{2}\right)}, \\ &= e^{-\beta\frac{\hbar\omega}{2}} \sum_{n=0}^{\infty} \left(e^{-\beta\hbar\omega}\right)^n, \\ &= e^{-\beta\frac{\hbar\omega}{2}} \left(\frac{1}{1 - e^{-\beta\hbar\omega}}\right), \\ &= \frac{1}{e^{\beta\hbar\omega/2} - e^{-\beta\hbar\omega/2}}, \\ &= \frac{1}{2\sinh(\beta\hbar\omega/2)}. \end{aligned} \tag{2.2.2}$$

Alternatively, the partition function can be expressed through the path integral formalism in Euclidean time. For the harmonic oscillator, it is defined as:

$$Z_{\text{H.O.}}(\beta) = \int_{q_E(0)=q_E(\beta)} \mathcal{D}q_E(\tau)\, e^{-S_E}, \tag{2.2.3}$$

where the Euclidean action S_E is

$$S_E = \frac{m}{2} \int_0^{\beta} d\tau \left(\left(\frac{dq_E(\tau)}{d\tau}\right)^2 + \omega^2 q_E^2(\tau)\right). \tag{2.2.4}$$

Since we must consider periodic trajectories with period β, we expand $q_E(\tau)$ in a Fourier series:

$$q_E(\tau) = \frac{1}{\beta} \sum_{n=-\infty}^{\infty} \tilde{q}_n e^{i\omega_n \tau}, \tag{2.2.5}$$

where $\omega_n = 2\pi n/\beta$ denotes the Matsubara frequencies.

2.2.1 Reality Conditions and Coefficients

Because the physical path $q_E(\tau) \in \mathbb{R}$, we must impose a reality condition on the Fourier coefficients. Starting from the inverse transform:

$$\tilde{q}_n = \int_0^\beta q_E(\tau) e^{-i\omega_n \tau} d\tau, \tag{2.2.6}$$

it follows that:

$$\tilde{q}_n^* = \int_0^\beta q_E(\tau) e^{i\omega_n \tau} d\tau = \int_0^\beta q_E(\tau) e^{-i(-\omega_n)\tau} d\tau = \tilde{q}_{-n}. \tag{2.2.7}$$

Under the condition $\tilde{q}_{-n} = \tilde{q}_n^*$, the terms of order $\pm n$ in Eq. (2.2.5) combine as follows:

$$\tilde{q}_n e^{i\omega_n \tau} + \tilde{q}_{-n} e^{-i\omega_n \tau} = 2\mathrm{Re}\{\tilde{q}_n e^{i\omega_n \tau}\} \in \mathbb{R}. \tag{2.2.8}$$

By decomposing the coefficients into real and imaginary parts as $\tilde{q}_n = a_n + ib_n$, where $a_n, b_n \in \mathbb{R}$, the reality condition from Eq. (2.2.7) implies:

$$a_n = a_{-n}, \quad b_n = -b_{-n}, \quad \text{and specifically } b_0 = 0. \tag{2.2.9}$$

2.2.2 Evaluating the Euclidean Action

To evaluate the integral in Eq. (2.2.3), we substitute the expansion from Eq. (2.2.5). First, we compute the time derivative:

$$\dot{q}_E(\tau) = \frac{i}{\beta} \sum_{n=-\infty}^{\infty} \omega_n \tilde{q}_n e^{i\omega_n \tau}. \tag{2.2.10}$$

Integrating the potential term $q_E^2(\tau)$ over the period β, we obtain:

$$\int_0^\beta \omega^2 q_E^2(\tau) d\tau = \frac{\omega^2}{\beta^2} \sum_{k,l} \tilde{q}_k \tilde{q}_l \int_0^\beta e^{i(\omega_k + \omega_l)\tau} d\tau. \tag{2.2.11}$$

Using the orthogonality property:

$$\int_0^\beta e^{i(\omega_k + \omega_l)\tau} d\tau = \beta \delta_{k,-l}, \tag{2.2.12}$$

the expression simplifies to:

$$\int_0^\beta \omega^2 q_E^2(\tau)d\tau = \frac{\omega^2}{\beta}\sum_{k=-\infty}^{\infty} \tilde{q}_k\tilde{q}_{-k} = \frac{\omega^2}{\beta}\sum_{k=-\infty}^{\infty} |\tilde{q}_k|^2 = \frac{\omega^2}{\beta}\sum_{k=-\infty}^{\infty} (a_k^2 + b_k^2). \quad (2.2.13)$$

Similarly, applying the derivative Eq. (2.2.10) and the orthogonality condition Eq. (2.2.12) to the kinetic term:

$$\begin{aligned}\int_0^\beta \dot{q}_E^2(\tau)d\tau &= -\frac{1}{\beta^2}\sum_{k,l} \omega_k\omega_l\tilde{q}_k\tilde{q}_l(\beta\delta_{k,-l}),\\ &= -\frac{1}{\beta}\sum_{k=-\infty}^{\infty} \omega_k(-\omega_k)\tilde{q}_k\tilde{q}_k^* = \frac{1}{\beta}\sum_{k=-\infty}^{\infty} \omega_k^2(a_k^2+b_k^2). \end{aligned} \quad (2.2.14)$$

Substituting Eqs. (2.2.13) and (2.2.14) into the Euclidean action S_E and using the symmetry conditions from Eq. (2.2.9), we find:

$$\begin{aligned} S_E &= \frac{m}{2}\int_0^\beta d\tau \left(\dot{q}_E^2 + \omega^2 q_E^2\right),\\ &= \frac{m}{2\beta}\sum_{k=-\infty}^{\infty} (\omega_k^2+\omega^2)(a_k^2+b_k^2),\\ &= \frac{m}{\beta}\sum_{k=1}^{\infty}(\omega_k^2+\omega^2)(a_k^2+b_k^2) + \frac{m\omega^2}{2\beta}a_0^2. \end{aligned} \quad (2.2.15)$$

2.2.3 Path Integral Measure and Partition Function

In the discretized time formalism, the transition amplitude is defined by the measure [see 26, p. 43]:

$$\int \mathcal{D}q = \lim_{n\to\infty}\left(\frac{m}{2\pi\hbar\epsilon}\right)^{n/2}\prod_{j=1}^{n-1} dq_j, \quad (2.2.16)$$

where $\epsilon = \beta/n$ is the lattice spacing in Euclidean time.

By transforming from the coordinates q_j to the Fourier coefficients a_n, b_n, the measure changes via a Jacobian $J = |\det(J)|$:

$$\int \mathcal{D}q_E = \lim_{n\to\infty}\left(\frac{m}{2\pi\hbar\epsilon}\right)^{n/2} J\int\left(\prod_{k=1}^{n-1} da_k db_k\right)da_0 = B(\beta)\int\left(\prod_{k=1}^{\infty} da_k db_k\right)da_0, \quad (2.2.17)$$

where we have absorbed the discrete normalization factor together with the Jacobian J into an overall constant $B(\beta)$. The dependence on β arises through the lattice spacing $\epsilon = \beta/n$, as well as from the normalization of the Fourier modes defined on the interval $[0, \beta]$. Substituting the action from Eq. (2.2.15) into the path integral Eq. (2.2.3), we obtain:

$$\begin{aligned} Z_{\text{H.O.}}(\beta) = B(\beta) \left(\int_{-\infty}^{+\infty} e^{-\frac{m\omega^2}{2\beta} a_0^2} \, da_0 \right) \prod_{k=1}^{\infty} \Bigg[\left(\int_{-\infty}^{+\infty} e^{-\frac{m}{\beta}(\omega_k^2+\omega^2)\, a_k^2} \, da_k \right) \\ \left(\int_{-\infty}^{+\infty} e^{-\frac{m}{\beta}(\omega_k^2+\omega^2) b_k^2} \, db_k \right) \Bigg], \qquad (2.2.18) \\ = B(\beta) \sqrt{\frac{2\pi\beta}{m\omega^2}} \prod_{k=1}^{\infty} \left(\sqrt{\frac{\pi\beta}{m(\omega_k^2+\omega^2)}} \right) \left(\sqrt{\frac{\pi\beta}{m(\omega_k^2+\omega^2)}} \right), \\ = B(\beta) \sqrt{\frac{2\pi\beta}{m\omega^2}} \prod_{k=1}^{\infty} \frac{\pi\beta}{m(\omega_k^2+\omega^2)}, \qquad (2.2.19) \end{aligned}$$

where each integral is taken over the full real line, reflecting the fact that the Fourier coefficients span $\mathbb{R}$, and we have used the standard Gaussian integral

$$\int_{-\infty}^{\infty} e^{-ax^2} dx = \sqrt{\frac{\pi}{a}}, \qquad a \in \mathbb{R}^+. \qquad (2.2.20)$$

Thus, the partition function for the harmonic oscillator is given by:

$$Z_{\text{H.O.}}(\beta) = B(\beta) \sqrt{\frac{2\pi\beta}{m\omega^2}} \prod_{k=1}^{\infty} \frac{\pi\beta}{m(\omega_k^2+\omega^2)}. \qquad (2.2.21)$$

At this stage, the expression appears to be divergent due to the infinite product over modes. However, this divergence is not physical: it originates from the overall normalization of the path integral, encoded in the factor $B(\beta)$, and from the infinite product itself, which requires regularization.

On the other hand, from the standard canonical approach, namely the definition of the partition function as a sum over energy eigenvalues (see Eq. (2.2.2)), we know that the result must be finite. Therefore, the apparent divergence signals that Eq. (2.2.21) is not yet properly normalized.

To recover the finite result, one must regularize the infinite product and fix the normalization factor $B(\beta)$ by matching to a known reference, such as the canonical partition function or an appropriate limiting case. For this purpose, we consider the free particle as the zero-frequency limit of the harmonic oscillator. In other words, the free-particle partition function is formally obtained from Eq. (2.2.21) by setting $\omega = 0$. However, this limit is subtle because the prefactor $\sqrt{2\pi\beta/(m\omega^2)}$ diverges due to the integration over the zero mode a_0.

Let us therefore analyze the partition function of the free particle directly.

The Euclidean action for the free particle is

$$S_E^F = \int_0^\beta \frac{m}{2}\dot{q}_E^2(\tau)\, d\tau. \tag{2.2.22}$$

From the Fourier expansion

$$q_E(\tau) = \frac{1}{\beta}\sum_{n=-\infty}^{\infty} \tilde{q}_n e^{i\omega_n\tau}, \tag{2.2.23}$$

with $\tilde{q}_n = a_n + ib_n$, it follows that

$$\int_0^\beta \dot{q}_E^2(\tau)\, d\tau = \frac{1}{\beta}\sum_{k=-\infty}^{\infty} \omega_k^2(a_k^2 + b_k^2), \tag{2.2.24}$$

and therefore

$$\begin{aligned}
S_E^F &= \int_0^\beta \frac{m}{2}\dot{q}_E^2(\tau)\, d\tau \\
&= \frac{m}{2\beta}\sum_{k=-\infty}^{\infty} \omega_k^2(a_k^2 + b_k^2), \\
&= \frac{m}{2\beta}\left(\sum_{k=-\infty}^{-1} \omega_k^2(a_k^2 + b_k^2) + \omega_0^2(a_0^2 + b_0^2) + \sum_{k=1}^{\infty}\omega_k^2(a_k^2 + b_k^2)\right), \\
&= \frac{m}{2\beta}\left(\sum_{k=1}^{\infty}\omega_{-k}^2(a_{-k}^2 + b_{-k}^2) + 0^2(a_0^2 + 0^2) + \sum_{k=1}^{\infty}\omega_k^2(a_k^2 + b_k^2)\right), \\
&= \frac{m}{\beta}\sum_{k=1}^{\infty}\omega_k^2(a_k^2 + b_k^2).
\end{aligned}$$

The free-particle partition function is obtained by inserting the action above into the Euclidean path integral and using the same functional measure introduced for the harmonic oscillator. Since the change of variables from the discretized coordinates q_j to the Fourier coefficients is identical, the measure again takes the form

$$\int \mathcal{D}q_E = \lim_{n\to\infty} \left(\frac{m}{2\pi\hbar\epsilon}\right)^{n/2} J \int \left(\prod_{k=1}^{n-1} da_k db_k\right) da_0 = B(\beta) \int \left(\prod_{k=1}^{\infty} da_k db_k\right) da_0. \tag{2.2.25}$$

The important difference with respect to the harmonic oscillator is that the free-particle action contains no term proportional to a_0^2. Therefore, the non-zero modes still give Gaussian integrals, while the zero mode must be treated separately. Substituting Eq. (2.2.23) into the path integral, we obtain

$$\begin{aligned}
Z^F &= \int_{q_E(0)=q_E(\beta)} \mathcal{D}q_E(\tau)\, e^{-S_E^F}, \\
&= B(\beta) \int \left(\prod_{k=1}^{\infty} da_k db_k\right) da_0 \exp\left[-\frac{m}{\beta}\sum_{k=1}^{\infty}\omega_k^2(a_k^2+b_k^2)\right], \\
&= B(\beta) \left(\int_{-\infty}^{+\infty} da_0\right) \prod_{k=1}^{\infty} \left(\int_{-\infty}^{+\infty} e^{-\frac{m}{\beta}\omega_k^2 a_k^2} da_k\right) \left(\int_{-\infty}^{+\infty} e^{-\frac{m}{\beta}\omega_k^2 b_k^2} db_k\right), \\
&= B(\beta) V \prod_{k=1}^{\infty} \left(\sqrt{\frac{\pi\beta}{m\omega_k^2}}\right) \left(\sqrt{\frac{\pi\beta}{m\omega_k^2}}\right), \\
&= B(\beta) V \prod_{k=1}^{\infty} \frac{\pi\beta}{m\omega_k^2}.
\end{aligned}$$

Here we have denoted by $V \equiv \int da_0$ the contribution of the translational zero mode. This factor deserves a brief comment: since the action of the free particle does not depend on the zero mode, the integration over a_0 does not produce a Gaussian factor; instead, it measures the volume associated with the translational invariance of the system. To make this statement precise, we place the particle in a box of length L, so that the spatial coordinate is restricted to the interval $[0, L]$. With the Fourier convention in Eq. (2.2.23), the zero mode is

$$a_0 = \tilde{q}_0 = \int_0^\beta q_E(\tau)\, d\tau = \beta\, \bar{q}, \tag{2.2.26}$$

where $\bar{q} \equiv \beta^{-1} \int_0^\beta q_E(\tau)\, d\tau$ is the average position along the Euclidean trajectory. Since $q_E(\tau) \in [0, L]$, it follows that $\bar{q} \in [0, L]$, and therefore the zero mode ranges over the interval $a_0 \in [0, \beta L]$. Hence,

$$\int da_0 = \beta \int_0^L d\bar{q} = \beta L. \tag{2.2.27}$$

In the decompactification limit $L \to \infty$, this factor diverges, as expected for the infinite translational volume of a free particle.

The ratio between the partition functions of the harmonic oscillator and the free particle is then

$$\begin{aligned}\frac{Z_{\text{H.O.}}}{Z_F} &= \frac{B(\beta)\sqrt{\frac{2\pi\beta}{m\omega^2}}\prod_{k=1}^{\infty}\frac{\pi\beta}{m(\omega_k^2+\omega^2)}}{B(\beta)\left(\int da_0\right)\prod_{k=1}^{\infty}\frac{\pi\beta}{m\omega_k^2}}, \\ &= \frac{1}{\int da_0}\sqrt{\frac{2\pi\beta}{m\omega^2}}\prod_{k=1}^{\infty}\frac{\omega_k^2}{\omega_k^2+\omega^2}. \end{aligned} \tag{2.2.28}$$

Using the result $\int da_0 = \beta L$, this becomes

$$\frac{Z_{\text{H.O.}}}{Z_F} = \frac{1}{\beta L}\sqrt{\frac{2\pi\beta}{m\omega^2}}\prod_{k=1}^{\infty}\frac{\omega_k^2}{\omega_k^2+\omega^2}. \tag{2.2.29}$$

To determine the overall normalization, we now evaluate the free-particle partition function in a box of length L from the canonical point of view. For a particle confined to an interval of size L, the energy levels are

$$E_n = \frac{\pi^2 n^2}{2mL^2}, \qquad n = 1, 2, 3, \ldots \tag{2.2.30}$$

so that

$$Z_F = \sum_{n=1}^{\infty} e^{-\beta\frac{\pi^2 n^2}{2mL^2}}. \tag{2.2.31}$$

In the large-L limit, the spacing between neighboring energy levels becomes small and the sum can be approximated by an integral,

$$Z_F \xrightarrow{L\to\infty} \int_0^{\infty} dn\; e^{-\beta\frac{\pi^2 n^2}{2mL^2}}. \tag{2.2.32}$$

Using Eq. (2.2.20) with $a = \beta\pi^2/(2mL^2)$, and noting that the integration range is $[0, \infty)$ rather than $(-\infty, \infty)$, one obtains an additional factor of $1/2$. Therefore,

$$Z_F = \frac{1}{2}\sqrt{\frac{2mL^2}{\pi\beta}}. \tag{2.2.33}$$

Substituting this result into the ratio above, we find

$$Z_{\text{H.O.}} = \frac{1}{\beta\omega} \prod_{k=1}^{\infty} \frac{\omega_k^2}{\omega_k^2 + \omega^2}. \tag{2.2.34}$$

Using the Matsubara frequencies $\omega_k = 2\pi k/\beta$, we obtain

$$\frac{\omega_k^2}{\omega_k^2 + \omega^2} = \frac{k^2}{k^2 + \tilde{\omega}^2}, \qquad \tilde{\omega} \equiv \frac{\beta\omega}{2\pi}. \tag{2.2.35}$$

Hence,

$$Z_{\text{H.O.}} = \frac{1}{\beta\omega} \prod_{k=1}^{\infty} \frac{k^2}{k^2 + \tilde{\omega}^2}. \tag{2.2.36}$$

We now apply the standard infinite-product identity

$$\prod_{k=1}^{\infty} \frac{k^2}{k^2 + \tilde{\omega}^2} = \frac{\pi\tilde{\omega}}{\sinh(\pi\tilde{\omega})} = \frac{\beta\omega/2}{\sinh(\beta\omega/2)}. \tag{2.2.37}$$

Substituting this expression into the previous equation gives

$$Z_{\text{H.O.}} = \frac{1}{\beta\omega} \frac{\beta\omega/2}{\sinh(\beta\omega/2)} = \frac{1}{2\sinh(\beta\omega/2)}. \tag{2.2.38}$$

This agrees precisely with the canonical result obtained in Eq. (2.2.2). Therefore, the path integral computation not only reproduces the expected answer, but also illustrates explicitly how the divergent normalization can be removed by taking the ratio with the free-particle partition function and regularizing the resulting infinite product. More importantly, this simple example makes transparent the ingredients that will reappear in the gravitational setting: the expansion around a classical background, the emergence of functional determinants from Gaussian integration, and the special role played by zero modes and normalization factors.

The harmonic oscillator is, of course, far simpler than the black hole backgrounds of interest, but that is precisely why it is useful. It provides a clean laboratory in which the logic of the semiclassical expansion can be displayed without the technical complications of diffeomorphism invariance, gauge constraints, and higher-curvature interactions. Once this logic is clear, the subsequent chapters can be read as a progressive elaboration of the same structure: first one identifies the relevant Einstein-Maxwell-Gauss-Bonnet saddle and its near-extremal throat, and then one studies the quadratic operators that control the one-loop fluctuations around it.

In this sense, the present chapter serves as the conceptual bridge between the formal definition of the Euclidean path integral and the concrete black hole computation developed in the rest of the thesis. The next chapter turns to the charged Einstein-Maxwell-Gauss-Bonnet solution itself and establishes the classical near-extremal background, while the subsequent one extracts the generalized Lichnerowicz operator and analyzes its zero modes.

Chapter 3

Einstein-Gauss-Bonnet coupled to Maxwell

3.1 The charged black hole in Einstein-Maxwell-Gauss Bonnet

Having established in the harmonic-oscillator example how the path integral reduces to Gaussian integrations and how its normalization can be fixed by comparison with a reference system, we now turn to the gravitational problem of interest. The Einstein-Maxwell-Gauss-Bonnet theory provides a concrete framework in which these ideas can be implemented for black-hole backgrounds and, eventually, for the computation of one loop corrections to the entropy.

The five-dimensional Einstein-Gauss-Bonnet theory coupled to a Maxwell field can be defined via the bulk action

$$I_{\text{bulk}}[g,A] = \frac{1}{\kappa^2}\int d^5x\sqrt{-g}\,(R-2\Lambda+\alpha\mathcal{G}-F_{\rho\sigma}F^{\rho\sigma})\,, \tag{3.1.1}$$

$$\mathcal{G} = R^{\mu\nu\rho\sigma}R_{\mu\nu\rho\sigma}-4R^{\mu\nu}R_{\mu\nu}+R^2, \tag{3.1.2}$$

with $\kappa^2 = 16\pi G$ and where $\mathcal{G}$ denotes the Gauss-Bonnet invariant.

Throughout this section we work in Lorentzian signature and adopt the mostly-plus convention.

For later use, it is also convenient to fix our definition of the Hodge dual. For a

p-form

$$F_p = \frac{1}{p!} F_{\mu_1 \dots \mu_p} \, dx^{\mu_1} \wedge \dots \wedge dx^{\mu_p} \tag{3.1.3}$$

on a D-dimensional manifold with metric $g_{\mu\nu}$ and determinant g, we define

$$\star F_p = \frac{\sqrt{|g|}}{p!(D-p)!} F^{\mu_1 \dots \mu_p} \, \epsilon_{\mu_1 \dots \mu_p \nu_1 \dots \nu_{D-p}} \, dx^{\nu_1} \wedge \dots \wedge dx^{\nu_{D-p}}, \tag{3.1.4}$$

with orientation fixed by $\epsilon_{x^1 \dots x^D} = 1$. In this section we restrict to $D = 5$.

The equations of motion derived from the action (3.1.1) are

$$d \star F = 0, \tag{3.1.5}$$

$$R_{\mu\nu} - \frac{1}{2} g_{\mu\nu} R + \Lambda g_{\mu\nu} + \alpha H_{\mu\nu} = 2 T_{\mu\nu}, \tag{3.1.6}$$

where the energy-momentum tensor of the Maxwell field is

$$T_{\mu\nu} = F_{\mu\lambda} F_\nu{}^\lambda - \frac{1}{4} g_{\mu\nu} F_{\lambda\delta} F^{\lambda\delta}, \tag{3.1.7}$$

and the contribution from the Gauss-Bonnet term is given by

$$H_{\mu\nu} = \frac{1}{\sqrt{-g}} \frac{\delta}{\delta g_{\mu\nu}} \int d^5 x \sqrt{-g} \, \mathcal{G}, \tag{3.1.8}$$

$$= 2 R R_{\mu\nu} - 4 R_{\mu\rho} R^\rho{}_\nu - 4 R^\delta{}_\rho R^\rho{}_{\mu\delta\nu} + 2 R_{\mu\rho\sigma\delta} R_\nu{}^{\rho\sigma\delta} - \frac{1}{2} \mathcal{G} g_{\mu\nu}. \tag{3.1.9}$$

A class of solutions to these equations is given by static, charged black holes with metric

$$ds^2 = -f(r) \, dt^2 + \frac{dr^2}{f(r)} + r^2 ds^2(S^3), \tag{3.1.10}$$

$$f(r) = 1 + \frac{r^2}{4\alpha} \left(1 - \sqrt{1 + \frac{4\alpha\Lambda}{3} + \frac{m\alpha}{r^4} - \frac{16 q^2 \alpha}{3 r^6}} \right), \tag{3.1.11}$$

and gauge potential

$$A = \frac{1}{\sqrt{2}} \left(\frac{q}{r^2} - \frac{q}{r_+^2} \right) dt. \tag{3.1.12}$$

Here, m is an integration constant related to the black hole mass, q is proportional to the electric charge, and r_+ denotes the radial coordinate of the event horizon, defined as the largest root of $f(r)$. We choose the branch of the solution that admits a smooth Einstein-Maxwell limit as $\alpha \to 0$. Expanding $f(r)$ for small α, one finds

$$f(r) = 1 - \frac{m}{r^2} + \frac{4q^2}{3r^4} - \frac{\Lambda}{6}r^2 + \mathcal{O}(\alpha), \tag{3.1.13}$$

which corresponds to the standard five-dimensional Reissner-Nordström-(A)dS solution. The asymptotic structure of the spacetime can be inferred from the large-r behavior of the metric function. Expanding $f(r)$ for $r \to \infty$, one obtains

$$f(r) = \frac{r^2}{\ell_{\text{eff}}^2} + 1 - \frac{3m}{8\sqrt{9+12\alpha\Lambda}\, r^2} + \frac{2q^2}{\sqrt{9+12\alpha\Lambda}\, r^4} + \mathcal{O}(r^{-6}) \ . \tag{3.1.14}$$

The leading term, proportional to r^2, determines the asymptotic geometry. In particular, for $\Lambda = 0$ one has $\ell_{\text{eff}} \to \infty$, and the spacetime becomes asymptotically flat. For $\Lambda \neq 0$, the metric approaches that of (anti-)de Sitter spacetime, but with an effective cosmological constant induced by the Gauss-Bonnet coupling. More precisely, the asymptotic curvature scale is governed by an effective AdS radius ℓ_{eff}, defined as

$$\ell_{\text{eff}}^2 = -\frac{3}{\Lambda}\left(1 + \sqrt{1 + \frac{4}{3}\alpha\Lambda}\right) \ . \tag{3.1.15}$$

This shows that higher-curvature corrections modify the relation between the cosmological constant and the curvature radius of the spacetime. In particular, even though Λ appears in the action, the asymptotic geometry is controlled by ℓ_{eff} rather than directly by Λ.

A well-defined action principle requires supplementing (3.1.1) with appropriate boundary terms. In particular, the bulk action alone does not lead to a well-posed variational principle, since variations of the metric generate normal derivatives at the boundary. To cancel these contributions, one must include the generalized Gibbons-Hawking-York (GHY) term appropriate for Einstein-Gauss Bonnet gravity [24, 27].

Moreover, in asymptotically AdS_5 spacetimes, the on-shell action generically diverges due to the infinite volume of the spacetime. These divergences can be removed by adding local covariant counterterms constructed from intrinsic boundary quantities [28–30]. The resulting renormalized action is finite and suitable for thermodynamic applications.

These contributions are respectively given by

$$I_{\rm GHY} = \frac{1}{\kappa^2}\int_{\partial M} d^4x\sqrt{-h}\left[2K + \alpha\delta^{abc}_{ijk}K^i{}_a\left(\frac{1}{2}\mathcal{R}^{jk}{}_{bc} - \frac{1}{3}K^j{}_bK^k{}_c\right)\right]\,, \tag{3.1.16}$$

$$I_{\rm ct} = \frac{2}{\kappa^2}\int_{\partial M} d^4x\sqrt{-h}\left[-\frac{1}{\ell_{\rm eff}}\left(2+\sqrt{1-\frac{8\alpha}{L^2}}\right) - \frac{\ell_{\rm eff}}{4}\left(2-\sqrt{1-\frac{8\alpha}{L^2}}\right)\mathcal{R}\right]\,, \tag{3.1.17}$$

where $\Lambda = -6/L^2 < 0$. Here, h_{ab} denotes the induced metric on the timelike boundary $\partial\mathcal{M}$ at fixed radial coordinate r, with topology $\mathbb{R}_t \times S^3$. The tensor K_{ab} is the extrinsic curvature associated with the outward-pointing unit normal to the boundary, $K = h^{ab}K_{ab}$ is its trace, and $\mathcal{R}$ is the Ricci scalar of the boundary $\partial\mathcal{M}$ constructed from h_{ab}.

Finally, in order to implement the canonical ensemble, corresponding to fixed temperature and electric charge in AdS, the action must be further supplemented by an additional boundary term. In the presence of a Maxwell field, fixing the charge rather than the potential requires performing a Legendre transform of the action, which is achieved by adding the Hawking-Ross term [31]:

$$I_{\rm HR} = \frac{4}{\kappa^2}\int_{\partial\mathcal{M}} d^4x\sqrt{-h}\,n_aF^{ab}A_b = \frac{4}{\kappa^2}\int_{\partial\mathcal{M}} A\wedge\star F\,. \tag{3.1.18}$$

Before turning to the thermodynamic analysis, it is useful to determine whether the charged solution admits an extremal limit.

3.1.1 Existence of an extremal branch

The near-extremal regime analyzed in the remainder of this work is meaningful only if the charged Einstein-Maxwell-Gauss-Bonnet solution admits extremal configurations. By definition, extremality occurs when the outer horizon becomes a double zero of the blackening factor. In other words, the horizon sits at a radius $r_+ \in \mathbb{R}_+$ such that

$$f(r_+) = 0\,, \qquad f'(r_+) = 0\,. \tag{3.1.19}$$

The first condition guarantees the existence of a Killing horizon, while the second ensures that the zero is degenerate. This is precisely the geometric signal that the outer and inner horizons have merged. Equivalently, the Hawking temperature vanishes, since from the general relation for metrics of the form (3.1.10), $T =$

$f'(r_+)/4\pi$, a double root immediately implies $T = 0$.

It is useful to emphasize why these conditions are non-trivial in the present theory. The metric function contains a non-linear term in the constants q and m, so requiring both $f(r_+) = 0$ and $f'(r_+) = 0$ does not merely fix the mass in terms of the charge, but selects special loci in parameter space where the two independent horizon conditions become compatible. Solving them simultaneously yields two algebraic branches, distinguished by the sign of $r_+^2 + 4\alpha$. This quantity appears naturally when differentiating $f(r)$ and therefore controls the local behavior of the solution near the degenerate horizon.

For $r_+^2 + 4\alpha > 0$, one finds

$$m = 16r_+^2 + 16\alpha - 4r_+^4\Lambda, \tag{3.1.20}$$

$$q^2 = \frac{r_+^4}{\sqrt{2}}(3 - r_+^2\Lambda), \tag{3.1.21}$$

together with

$$f''(r_+) = \frac{8 - 4r_+^2\Lambda}{r_+^2 + 4\alpha}. \tag{3.1.22}$$

This branch has a clear physical interpretation. For the range of interest in this work, $\Lambda \leq 0$, the factor $3 - r_+^2\Lambda$ in (3.1.21) is strictly positive for any real r_+, so $q^2 > 0$ automatically. Moreover, if $\alpha \geq 0$, then $r_+^2 + 4\alpha > 0$ is satisfied for every positive horizon radius. Hence this branch is not only algebraically allowed but also naturally realized in the parameter region continuously connected to standard Einstein-Maxwell theory. The expression (3.1.22) for the second derivative is likewise positive in this regime, because both numerator and denominator are positive, showing that the degenerate zero is a local minimum of $f(r)$. This is the expected behavior for an extremal black hole, where the double root separates the exterior region from the would-be interior.

On the other hand, for $r_+^2 + 4\alpha < 0$, one obtains

$$q^2 = \frac{3r_+^6 + 6r_+^4\alpha + 2r_+^6\alpha\Lambda}{-2\alpha}, \tag{3.1.23}$$

$$m = 16\alpha - \frac{4r_+^4(1 + \alpha\Lambda)}{\alpha}, \tag{3.1.24}$$

and

$$f''(r_+) = \frac{4\left[2\alpha + r_+^2(1+\alpha\Lambda)\right]}{\alpha(r_+^2+4\alpha)}. \tag{3.1.25}$$

This second branch is much less compelling for our purposes. First, it requires $\alpha < 0$ and in particular $r_+^2 < -4\alpha$, so it has no smooth counterpart in the Einstein Maxwell limit $\alpha \to 0$. Second, the positivity of q^2 is no longer automatic and depends on a more restrictive balance among r_+, α, and Λ. Thus, although it solves the extremality equations algebraically, it does not provide the robust physical branch needed for a controlled near-extremal expansion around the General Relativity regime.

In what follows, we therefore restrict our attention to the first branch. It is the one continuously connected to the Einstein Maxwell limit as $\alpha \to 0$, it guarantees a real positive charge for $\Lambda \leq 0$, and it exhibits the correct local structure of an extremal horizon. This is the branch that underlies the extremal background relevant for the subsequent near-extremal analysis. The next step is to rewrite the solution in a way that makes the coexistence and eventual merger of the outer and inner horizons fully explicit.

3.2 Thermodynamic Quantities

In order to perform the subsequent thermodynamic analysis, it is convenient to rewrite the metric function $f(r)$ in terms of the inner and outer horizons, r_- and r_+. This can be achieved by exploiting the polynomial structure underlying the horizon condition.

Imposing $f(r_+) = 0$ is equivalent to requiring that r_+ is a root of the polynomial

$$P(r) = \Lambda r^6 - 6r^4 + \frac{3}{4}(m - 16\alpha)r^2 - 4q^2\,. \tag{3.2.1}$$

Due to the fact that $P(r)/f(r)$ is function of r^2, the roots of $P(r)$ come in pairs $\{\pm r_i\}$, and can be parameterized as

$$\{r_+,\, r_-,\, r_3,\, -r_+,\, -r_-,\, -r_3\}\,. \tag{3.2.2}$$

Here, r_3 does not correspond to a physical horizon in general, but rather arises from the algebraic structure of the polynomial.

Applying Vieta's formulas to the polynomial (3.2.1), one obtains relations between the roots and the coefficients of the polynomial. In particular, the non-trivial relations can be written as

$$r_+^2 + r_-^2 + r_3^2 = \frac{6}{\Lambda}\,, \tag{3.2.3}$$

$$r_+^2 r_-^2 + r_+^2 r_3^2 + r_-^2 r_3^2 = \frac{3}{4\Lambda}(m - 16\alpha)\,, \tag{3.2.4}$$

$$r_+^2 r_-^2 r_3^2 = \frac{4q^2}{\Lambda}\,. \tag{3.2.5}$$

These relations allow one to eliminate r_3 and express the parameters m and q entirely in terms of the horizon radii $r_\pm$. Solving for r_3^2 from (3.2.3) and substituting into (3.2.4) and (3.2.5), one finds

$$m = 16\alpha + 8(r_+^2 + r_-^2) - \frac{4\Lambda}{3}(r_+^4 + r_+^2 r_-^2 + r_-^4)\,, \tag{3.2.6}$$

$$q^2 = \frac{3}{2} r_+^2 r_-^2 - \frac{\Lambda}{4} r_+^2 r_-^2 (r_+^2 + r_-^2)\,. \tag{3.2.7}$$

Substituting these expressions back into the metric function, and eliminating r_3, it is possible to rewrite $f(r)$ in a form that makes its polynomial structure manifest. To this end, it is convenient to express the argument of the square root as

$$R(r) = 1 + \frac{4}{3}\Lambda\alpha + \frac{m\alpha}{r^4} - \frac{16}{3}\frac{q^2\alpha}{r^6}\,. \tag{3.2.8}$$

A straightforward algebraic manipulation shows that this expression can be reorganized as

$$R(r) = \left(1 + \frac{4\alpha}{r^2}\right)^2 + \frac{4\alpha}{3r^6} P(r)\,, \tag{3.2.9}$$

where $P(r)$ is the polynomial defined above.

Using the factorized form

$$P(r) = \Lambda(r^2 - r_+^2)(r^2 - r_-^2)(r^2 - r_3^2)\,, \tag{3.2.10}$$

the metric function can be written as

$$f(r) = 1 + \frac{r^2}{4\alpha}\left[1 - \sqrt{\left(1 + \frac{4\alpha}{r^2}\right)^2 + \frac{4\alpha\Lambda}{3r^6}(r^2 - r_+^2)(r^2 - r_-^2)(r^2 - r_3^2)}\right]\,. \tag{3.2.11}$$

Finally, eliminating r_3 through the Vieta relation

$$r_3^2 = \frac{6}{\Lambda} - r_+^2 - r_-^2\,, \tag{3.2.12}$$

one obtains an expression for $f(r)$ entirely in terms of the horizon radii $r_\pm$:

$$f(r) = 1+\frac{r^2}{4\alpha}\left[1-\sqrt{\left(1+\frac{4\alpha}{r^2}\right)^2+\frac{4\alpha\Lambda}{3r^6}(r^2-r_+^2)(r^2-r_-^2)\left(r^2-\left(\frac{6}{\Lambda}-r_+^2-r_-^2\right)\right)}\right]. \tag{3.2.13}$$

This representation makes explicit the role of the horizon radii and is particularly useful for computing thermodynamic quantities. Most importantly, it makes transparent how extremality is encoded in the horizon data: the limit $r_+ \to r_-$ corresponds to the coalescence of the two physical horizons.

The first quantity to examine is the Hawking temperature, since it directly measures how far the solution lies from extremality. In this parametrization, it takes the form

$$T = \frac{f'(r_+)}{4\pi} = \frac{(r_+^2 - r_-^2)(6 - 2\Lambda r_+^2 - \Lambda r_-^2)}{12\pi r_+(r_+^2 + 4\alpha)}. \tag{3.2.14}$$

Having identified the temperature, the next thermodynamic observable of interest is the entropy. In a higher-curvature theory this quantity cannot be read off from the area law alone, so one must instead use Wald's formula [32, 33], which associates an entropy to any stationary horizon as a Noether charge. For a diffeomorphism-invariant theory, the entropy is given by

$$S = -2\pi \int_{\mathcal{H}} d^3x\sqrt{h}\, \frac{\partial \mathcal{L}}{\partial R_{\mu\nu\rho\sigma}}\epsilon_{\mu\nu}\epsilon_{\rho\sigma}\,, \tag{3.2.15}$$

where $\mathcal{H}$ denotes a spatial cross-section of the horizon, h is the induced metric on $\mathcal{H}$, and $\epsilon_{\mu\nu}$ is an antisymmetric tensor constructed from the two independent normal directions to $\mathcal{H}$ at each point. It characterizes the two-dimensional plane orthogonal to the horizon cross-section..

Applying this formula to the Einstein-Gauss-Bonnet theory (3.1.1), one finds that the entropy receives a correction proportional to the Gauss-Bonnet coupling α. For the static, spherically symmetric solution, taking $\xi = \partial_t$ and evaluating the expression at the outer horizon $r = r_+$, the entropy becomes

$$S = \frac{\pi^2 r_+^3}{2G}\left(1 + \frac{12\alpha}{r_+^2}\right) . \tag{3.2.16}$$

The expression above shows that the entropy does not follow the standard Bekenstein Hawking area law, but instead receives corrections proportional to the Gauss-Bonnet coupling. In particular, both terms r_+^3 and αr_+ have the same dimension and contribute on equal footing. Equivalently, the entropy can be written as

$$S = \frac{A}{4G}\left(1 + \frac{12\alpha}{r_+^2}\right) , \tag{3.2.17}$$

where $A = 2\pi^2 r_+^3$ is the area of the horizon. This shows that higher-curvature corrections modify the Bekenstein-Hawking area law by introducing a term proportional to the intrinsic curvature scale of the horizon.

Another useful quantity in the canonical ensemble is the heat capacity at fixed charge,

$$C_q = T\left(\frac{\partial S}{\partial T}\right)_q . \tag{3.2.18}$$

Using the temperature and entropy above, one obtains

$$C_q = \frac{3\pi^2 r_+ (r_+^2 + 4\alpha)^2 \left(3r_+^4 - \Lambda r_+^6 - 2q^2\right)}{2G\left(-\Lambda r_+^8 - 12\alpha\Lambda r_+^6 - 3r_+^6 + 12\alpha r_+^4 + 10q^2 r_+^2 + 24\alpha q^2\right)} . \tag{3.2.19}$$

This expression measures the local thermal response of the black hole at fixed electric charge.

With the temperature, entropy, and heat capacity at hand, one can complete the thermodynamic description by identifying the conserved charges and their conjugate potentials. With this normalization, the conserved charges of the solution can be defined in such a way that the first law of black hole thermodynamics,

$$dM = TdS + \Phi dQ , \tag{3.2.20}$$

is satisfied.

The electric charge can be obtained from the Maxwell sector of the theory by considering the associated conserved current. Starting from the action

$$I[A] = -\frac{2}{\kappa^2}\int F \wedge \star F\,, \tag{3.2.21}$$

the variation with respect to the gauge field yields the equations of motion $d \star F = 0$, which imply the existence of a conserved charge. The electric charge is then defined as the flux of the electric field through a spatial section Σ at infinity,

$$Q = \frac{4}{\kappa^2}\int_{\partial\Sigma} \star F\,. \tag{3.2.22}$$

For the static, spherically symmetric solution under consideration, this expression evaluates to

$$Q = -\frac{\pi q}{\sqrt{2}G}\,. \tag{3.2.23}$$

The chemical potential Φ is defined as the difference of the electric potential between the horizon and infinity, yielding

$$\Phi = -\frac{q}{\sqrt{2}r_+^2}\,. \tag{3.2.24}$$

The mass of the configuration is obtained from the asymptotic behavior of the metric and is given by

$$M = \frac{3\pi m}{64G}\,. \tag{3.2.25}$$

In the following, we will use the pairs (m, M) and (q, Q) interchangeably, depending on convenience. At this stage, all thermodynamic quantities have been expressed in terms of the horizon radii, so the extremal limit can now be implemented directly by taking the degenerate-horizon condition $r_+ = r_-$.

In the canonical ensemble, where the charge Q is held fixed, the existence of the extremal branch implies a minimum mass $M = M_{\mathrm{ext}}(Q)$ at which the inner and outer horizons coincide, $r_0 := r_+ = r_-$. This statement follows directly from the temperature formula (3.2.14): at fixed charge and for $r_+^2 + 4\alpha > 0$, the vanishing of T is achieved precisely when $r_+ = r_-$. Evaluating (3.2.6) on this locus then gives the corresponding extremal mass parameter,

$$m_{\mathrm{ext}} = 16r_0^2(q) + 16\alpha - 4r_0^4(q)\Lambda\,. \tag{3.2.26}$$

While the charge constraint is obtained from (3.2.7) evaluated on the same degenerate configuration. The extremal radius r_0 can therefore be expressed purely in terms of the charge parameter q. Solving (3.2.7) for r_0 through Cardano's formula gives

$$r_0^2(q) = \frac{1}{\Lambda}\left[1 + 2\cos\left(\frac{1}{3}\arccos(1 - q^2\Lambda^2) + \frac{2n\pi}{3}\right)\right], \qquad \Lambda \neq 0\,, \tag{3.2.27}$$

$$r_0^2(q) = \sqrt{\frac{2}{3}}|q|\,, \qquad \Lambda = 0\,, \tag{3.2.28}$$

where $n = 0, 1, 2, \ldots,$ and r_0 is defined as the largest real root. In this way, extremality is not merely assumed but completely characterized by the pair of algebraic relations above: for each fixed charge in the physical branch, they determine the degenerate horizon radius and the corresponding minimum mass.

Once the extremal solution has been identified, near-extremal configurations are conveniently described by a small-temperature expansion around $T = 0$ at fixed charge. Writing the energy as $M = M(T, Q)$ and expanding around extremality, one finds

$$m = m_{\rm ext} - \frac{16\pi^2(r_0^2 + 4\alpha)^2}{r_0^2\Lambda - 2}T^2 + \mathcal{O}(T^3)\,, \tag{3.2.29}$$

or equivalently

$$M = M_{\rm ext}(Q) + \frac{T^2}{M_{\rm gap}} + \mathcal{O}(T^3)\;, \tag{3.2.30}$$

The absence of a linear term in T is the key feature here: once the charge is held fixed, the first correction to the extremal energy is quadratic. It is therefore natural to parametrize this leading departure from extremality in terms of a mass gap, defined by

$$M_{\rm gap} := \frac{4G(2 - \Lambda r_0^2)}{3\pi^3(4\alpha + r_0^2)^2}\,. \tag{3.2.31}$$

Since we are considering $\Lambda \leq 0$, the mass gap $M_{\rm gap}$ is strictly positive. This is another explicit example where the expression (1.0.7) from the introduction holds. As a consequence, deviations from extremality at fixed charge and low temperature follow the same qualitative behavior as in General Relativity: the energy above the extremal bound scales quadratically with the temperature,

$$M - M_{\text{ext}} \sim \mathcal{O}(T^2)\,. \tag{3.2.32}$$

As discussed in the Introduction, this has an important physical implication. The typical energy of a Hawking quantum is of order T, whereas the excess energy available above extremality behaves as T^2. Therefore, at sufficiently low temperatures, the system does not possess enough energy to emit even a single Hawking quantum. In this regime, the black hole becomes effectively stable against thermal radiation.

This behavior suggests that the density of states is sharply peaked around the extremal configuration. Indeed, the extremal black hole can carry a macroscopic entropy, implying a large degeneracy of microstates at zero temperature. The existence of a finite mass gap then separates this highly degenerate ground state from the first excited states that can participate in thermal radiation. Such a structure often hints at an underlying symmetry that enhances the degeneracy of the extremal configuration, as occurs in certain supersymmetric or supergravity settings.

However, in close analogy with the Einstein-Maxwell case, no such symmetry is currently known in Einstein-Gauss-Bonnet-Maxwell theory that could account for this large, gapped ground-state degeneracy. This constitutes a well-known puzzle in black hole physics [6–8], now extended to the higher-curvature setting considered here.

For later convenience, we also denote the same quantity by

$$E_{\text{gap}} = \frac{4G(2-\Lambda r_0^2)}{3\pi^3(4\alpha + r_0^2)^2}\,, \tag{3.2.33}$$

which explicitly depends on the Gauss Bonnet coupling α. For small α, this expression departs from its General Relativity counterpart by a correction that is linear in α, reflecting the impact of higher-curvature interactions on the near-extremal spectrum.

Further insight comes from analyzing the first law of thermodynamics in the canonical ensemble. Considering two infinitesimally close equilibrium configurations at fixed charge, one has

$$\delta M = T\,\delta S\,. \tag{3.2.34}$$

From this relation, it follows that in order to generate a contribution to the energy that is linear in T at low temperatures, thereby allowing for Hawking emission at arbitrarily small T, the entropy must contain a term logarithmic in the temperature, $\sim \log T$.

In General Relativity, it has been shown that such logarithmic contributions arise from quantum corrections to the semiclassical Bekenstein Hawking entropy, in particular from one loop effects in the Euclidean path integral [34–43]. These corrections modify the low temperature thermodynamics and can, in principle, lift the strict mass gap present at the classical level.

Motivated by these considerations, we now turn to the near-horizon, near-extremal regime. A full one loop computation on the complete black-hole geometry is prohibitively complicated, whereas the near-horizon region isolates the degrees of freedom that dominate the low temperature dynamics while retaining the information relevant for the logarithmic corrections. The idea is therefore to zoom into the throat that develops as $T \to 0$, where the classical extremal structure derived above organizes the quantum problem most efficiently. Now, we determine the near-horizon geometry of the near-extremal solution, which furnishes the appropriate background for the quantum analysis.

3.3 Near-Horizon, Near-Extremal Geometry

The Euclidean near-horizon geometry of the near-extremal solution is obtained by expanding the spacetime around the $T = 0$ limit. To this end, we introduce the coordinate transformation

$$r = r_+(T) + 4\pi\ell_{\mathrm{AdS}}^2 T \sinh^2\left(\frac{\eta}{2}\right) \quad , \quad t = -\frac{i\tau}{2\pi T}\,, \tag{3.3.1}$$

with

$$\ell_{\mathrm{AdS}}^2 = \frac{r_0^2 + 4\alpha}{2(2 - \Lambda r_0^2)}, \quad \text{and } \tau \text{ the Euclidean time.} \tag{3.3.2}$$

In the strict $T \to 0$ limit, this transformation decouples an infinite AdS_2 throat with curvature radius ℓ_{AdS} from the rest of the spacetime. This is the geometric counterpart of the thermodynamic statement established above: as the temperature approaches zero at fixed charge, the solution develops a universal throat governed by the extremal radius r_0. At first order in the low temperature expansion, the geometry describes the near-horizon region of a near-extremal black hole and takes the form

$$g_{\mu\nu} = \bar{g}_{\mu\nu} + \delta g_{\mu\nu} T + \mathcal{O}(T^2) \,, \tag{3.3.3}$$

with the leading $\mathrm{AdS}_2 \times S^3$ spacetime given by

$$\bar{g}_{\mu\nu} dx^\mu dx^\nu = ds^2(\mathrm{AdS}_2) + r_0^2 ds^2(\mathrm{S}^3) \,. \tag{3.3.4}$$

Using the coordinates (τ, η) for the Euclidean AdS_2 space and (θ, ϕ, ψ) for the S^3, the line elements in (3.3.4) are respectively. The AdS_2 factor is written here in Euclidean Rindler-like coordinates; for a brief summary of its embedding and of its relation to other coordinate patches, see Appendix A.

$$ds^2(\mathrm{AdS}_2) = \ell_{\mathrm{AdS}}^2 (\sinh^2 \eta d\tau^2 + d\eta^2) \,, \tag{3.3.5}$$

$$ds^2(\mathrm{S}^3) = \frac{1}{4}(d\theta^2 + \sin^2\theta d\phi^2) + \frac{1}{4}(d\psi + \cos\theta d\phi)^2 \,. \tag{3.3.6}$$

The deformation at leading order in T is given by

$$\begin{aligned} \delta g_{\mu\nu} dx^\mu dx^\nu = 2\pi \ell_{\mathrm{AdS}}^2 \frac{[\ell_{\mathrm{AdS}}^2 (6 - r_0^2 \Lambda) + 3 r_0^2]}{3 r_0 (2 - r_0^2 \Lambda)} (2 + \cosh\eta) \tanh^2\left(\frac{\eta}{2}\right) (-\sinh^2\eta \, d\tau^2 + d\eta^2) \\ + 4\pi \ell_{\mathrm{AdS}}^2 \, r_0 \cosh\eta \, d\Omega_3^2. \end{aligned} \tag{3.3.7}$$

It is worth emphasizing that the resulting geometry depends on the Gauss-Bonnet coupling α exclusively through the AdS_2 curvature radius ℓ_{AdS} defined in (3.3.2). In particular, once the charge q is held fixed, the remaining coefficients of the solution are insensitive to variations in α, so that all higher-curvature effects are effectively encoded in the scale of the AdS_2 factor. This observation is conceptually important for what follows: although the full five-dimensional theory contains non-trivial higher-curvature interactions, in the near-horizon region their leading effect is funneled into a small set of effective parameters.

The expansion extends naturally to the gauge sector. Writing the gauge field as $A' = \overline{A} + \delta A\, T$, one finds

$$\overline{A} = \frac{\ell_{\rm AdS}^2}{r_0}\sqrt{3 - r_0^2\Lambda}\,(\cosh\eta - 1)\, i\, d\tau, \tag{3.3.8}$$

$$\delta A = -\frac{3\pi\ell_{\rm AdS}^4}{r_0^2}\sqrt{3 - \Lambda r_0^2}\,\sinh^2\eta\, i\, d\tau. \tag{3.3.9}$$

The corresponding field strength $\overline{F} = d\overline{A}$ is proportional to the volume form of the AdS_2 factor appearing in (3.3.4), reflecting the fact that the background gauge field is supported entirely along the AdS_2 directions. Moreover, the potential $\overline{A}$ is regular at the origin, namely, A_τ vanishes at $\eta = 0$.

Regularity of the Euclidean geometry at this point imposes a periodic identification of the Euclidean time coordinate, $\tau \sim \tau + 2\pi$. This condition ensures the absence of conical singularities and, at the same time, provides the appropriate setting for a mode decomposition of fields on the near-horizon background.

The geometry described in (3.3.3) should be understood as a perturbative solution of the Einstein-Gauss-Bonnet equations coupled to a Maxwell field, valid up to $\mathcal{O}(T^2)$. In constructing this expansion, we have imposed that the charge parameter q in (3.2.7) remains fixed along the deformation parameterized by T. This requirement uniquely determines the positions of the outer and inner horizons, r_+ and r_-, as functions of T. In other words, the near-extremal deformation is not arbitrary: it follows the canonical ensemble trajectory away from the extremal point while staying within the same charge sector.

More explicitly, the location of the event horizon admits the expansion shown in Appendix B.1:

$$\begin{aligned} r_+(T) &= r_0 + 2\pi\ell_{\rm AdS}^2 T + \pi^2\ell_{\rm AdS}^2\left(\frac{4(6 - r_0^2\Lambda)\alpha + 14r_0^2 - 5\Lambda r_0^4}{r_0(2 - \Lambda r_0^2)^2}\right)T^2 \\ &\quad + \frac{8\ell_{\rm AdS}^2\pi^3}{3r_0^2(2 - \Lambda r_0^2)^4}\Big[(96 + 32r_0^2\Lambda - 16r_0^4\Lambda^2)\alpha^2 + (168r_0^2 - 68r_0^4\Lambda + 4r_0^6\Lambda^2)\alpha \\ &\quad + 48r_0^4 - 31r_0^6\Lambda + 5r_0^8\Lambda^2\Big]T^3 + \mathcal{O}(T^4), \end{aligned} \tag{3.3.10}$$

while the Cauchy horizon is given by

$$
\begin{aligned}
r_-(T) = r_0 - 2\pi\ell_{\text{AdS}}^2 T - \pi^2\ell_{\text{AdS}}^2 \left(\frac{4(6-r_0^2\Lambda)\alpha + 30r_0^2 - 13r_0^4\Lambda}{3r_0(2-\Lambda r_0^2)^2}\right) T^2 \\
+ \frac{4\ell_{\text{AdS}}^2\pi^3}{9(2-\Lambda r_0^2)^4}\Big[(-384\Lambda + 112r_0^2\Lambda^2)\alpha^2 + (-432 + 120r_0^2\Lambda + 8r_0^4\Lambda^2)\alpha \\
- 180r_0^2 + 126r_0^4\Lambda - 23r_0^6\Lambda^2\Big]T^3 + \mathcal{O}(T^4).
\end{aligned}
\tag{3.3.11}
$$

These expressions will play a central role in what follows. In particular, they provide the precise dependence of the horizon data on the near-extremality parameter T, which is required in order to consistently evaluate the one-loop partition function around the near-horizon geometry. The explicit control over this expansion ensures that quantum fluctuations can be systematically incorporated while maintaining a fixed charge sector, a feature that will be essential in the computation of logarithmic corrections to the entropy. In this sense, the present section closes the classical part of the construction: it identifies the relevant extremal solution, characterizes its low temperature deformations, and furnishes the background on which the quantum analysis will be built.

Chapter 4

The generalized Lichnerowicz operator and its zero modes

4.1 Saddle-point approximation

The previous chapter identified the classical background that will play the central role in the quantum analysis: an extremal Einstein-Maxwell-Gauss-Bonnet black hole together with its controlled near-extremal deformation. Having isolated the relevant near-horizon throat and characterized its dependence on the temperature and charge, we are now in a position to study the fluctuations that govern the one loop partition function.

The strategy is the standard saddle-point one. The Euclidean path integral is expanded around the classical near-horizon solution, and the leading quantum correction is encoded in the Gaussian integral over linearized perturbations. Consequently, the first task is to expand the action (3.1.1) up to second order in the field perturbations. This requires evaluating the action on configurations where both the metric and the gauge field are perturbed around their background values.

To this end, we consider a non-compact, five-dimensional Lorentzian manifold M endowed with a metric $g'_{\mu\nu}$, defined as a perturbation of a fixed background metric $g_{\mu\nu}$ by a small fluctuation $h_{\mu\nu}$, namely

$$g'_{\mu\nu} = g_{\mu\nu} + h_{\mu\nu}\,. \tag{4.1.1}$$

Similarly, the gauge field is expanded around its background configuration A_μ by introducing a perturbation a_μ, such that

$$A'_\mu = A_\mu + a_\mu \,. \tag{4.1.2}$$

Using (4.1.1) and (4.1.2), the functional Taylor expansion for the action reads

$$\begin{aligned} I[g+h, A+a] &= I[g,A] + \int d^5x \left(\frac{\delta I}{\delta g_{\mu\nu}(x)} h_{\mu\nu}(x) + \frac{\delta I}{\delta A_\mu(x)} a_\mu(x) \right) \\ &+ \frac{1}{2} \int d^5x \int d^5y \left(h_{\mu\nu}(x) \frac{\delta^2 I}{\delta g_{\mu\nu}(x) \delta g_{\rho\sigma}(y)} h_{\rho\sigma}(y) + a_\mu(x) \frac{\delta^2 I}{\delta A_\mu(x) \delta g_{\rho\sigma}(y)} h_{\rho\sigma}(y) \right. \\ &\left. + h_{\mu\nu}(x) \frac{\delta^2 I}{\delta g_{\mu\nu}(x) \delta A_\rho(y)} a_\rho(y) + a_\mu(x) \frac{\delta^2 I}{\delta A_\mu(x) \delta A_\nu(y)} a_\nu(y) \right) + \dots \,. \end{aligned} \tag{4.1.3}$$

The zeroth-order term gives the classical on-shell action of the background, the first-order term vanishes because the background is a saddle point of the action, and the second-order term determines the fluctuation operator whose determinant yields the one loop correction. For this reason, we extract the quadratic form implicit in (4.1.3).

4.2 Quadratic fluctuations for Einstein-Gauss-Bonnet-Maxwell theory

We now compute (4.1.3) for the Einstein-Maxwell-Gauss-Bonnet theory. Since several sectors contribute and mix at quadratic order, it is useful to split the calculation into manageable pieces. For this purpose, and for clarity, we decompose the total action (3.1.1) as

$$I[g,A] = I_R[g] + I_\Lambda[g] + I_A[g,A] + I_{\mathcal{G}}[g] \,, \tag{4.2.1}$$

where

$$I_R[g] = \frac{1}{\kappa^2}\int d^5x\sqrt{-g}R + \frac{1}{\kappa^2}\int_{\partial\mathcal{M}} 2K\,\bar{\star}1\,, \tag{4.2.2}$$

$$I_\Lambda[g] = \frac{1}{\kappa^2}\int d^5x\sqrt{-g}(-2\Lambda)\,, \tag{4.2.3}$$

$$I_A[g,A] = \frac{1}{\kappa^2}\int d^5x\sqrt{-g}(-F_{\mu\nu}F^{\mu\nu}) + \frac{4}{\kappa^2}\int_{\partial\mathcal{M}} A\wedge\star F\,, \tag{4.2.4}$$

$$I_{\mathcal{G}}[g] = \frac{1}{\kappa^2}\int d^5x\sqrt{-g}\;\alpha\mathcal{G} + \frac{1}{\kappa^2}\int_{\partial\mathcal{M}} \alpha\delta^{abc}_{def}K^d{}_a\left(\frac{1}{2}\mathcal{R}^{ef}{}_{bc} - \frac{1}{3}K^e{}_bK^f_c\right)\bar{\star}1\,, \tag{4.2.5}$$

Where $\bar{\star}$ denotes the Hodge dual on $\partial\mathcal{M}$.

This background satisfies Dirichlet boundary conditions for the metric and Neumann boundary conditions for the gauge field, the latter being required to implement the canonical ensemble. As a result, the linear terms in the expansion (4.1.3) vanish upon imposing the equations of motion. This is precisely what makes the Gaussian approximation meaningful: once the saddle is fixed, the leading quantum information is entirely contained in the second variation.

The first functional derivatives of each contribution in (4.1.3) are given by

$$\frac{\delta I_R}{\delta g_{\mu\nu}(x)} = -\frac{\sqrt{-g}}{\kappa^2}G^{\mu\nu}\,, \qquad \frac{\delta I_\Lambda}{\delta g_{\mu\nu}(x)} = -\frac{\sqrt{-g}}{\kappa^2}\Lambda g^{\mu\nu}\,, \tag{4.2.6}$$

$$\frac{\delta I_A}{\delta A_\mu(x)} = \frac{4\sqrt{-g}}{\kappa^2}\nabla_\rho F^{\rho\mu}\,, \qquad \frac{\delta I_{\mathcal{G}}}{\delta g_{\mu\nu}(x)} = -\frac{\alpha\sqrt{-g}}{\kappa^2}H^{\mu\nu}\,, \tag{4.2.7}$$

$$\frac{\delta I_A}{\delta g_{\mu\nu}(x)} = \frac{\sqrt{-g}}{\kappa^2}\left(-\frac{1}{2}g^{\mu\nu}F_{\rho\sigma}F^{\rho\sigma} + 2F^\mu{}_\lambda F^{\nu\lambda}\right) \equiv \frac{2\sqrt{-g}}{\kappa^2}T^{\mu\nu}\,. \tag{4.2.8}$$

Note that all boundary contributions vanish by virtue of the imposed boundary conditions, together with the inclusion of the appropriate boundary terms in (4.2.2), (4.2.4), and (4.2.5).

For simplicity, we treat the computation of each contribution in the sum (4.2.1) separately. This decomposition also helps to clarify where the generalized Lichnerowicz operator will emerge: it is not inserted by hand, but rather appears as the natural differential operator governing the quadratic metric fluctuations.

To this end, we introduce the notation

$$I^{(f,g)} := \frac{1}{2}\int d^5x \int d^5y\, f_M(y)\, \frac{\delta^2 I}{\delta F_M(y)\, \delta G_N(x)}\, g_N(x)\,, \tag{4.2.9}$$

where F_M and G_N denote collective field labels, with $F_M, G_N \in \{A_\mu, g_{\mu\nu}\}$, while f_M and g_N denote the corresponding fluctuations, with $f_M, g_N \in \{a_\mu, h_{\mu\nu}\}$.

In the following, we compute each term $I^{(f,g)}$ appearing in the expansion (4.1.3). Once these pieces are assembled, the structure of the quadratic action will become transparent and the analysis of zero modes can be formulated in a precise operator language.

4.2.1 Computation of $I^{(h,h)}$ terms

4.2.1.1 Einstein Hilbert sector

We begin with the gravitational sector. Since this is the simplest place where the structure of the quadratic operator already becomes visible, it is useful to proceed step by step: first we vary the action once, then we vary the result again, and finally we reorganize the answer into a geometrically transparent form. The action is given by

$$I_R[g] = \frac{1}{16\pi G}\int_M d^5x\sqrt{-g}\, R + I_{BT}\,, \tag{4.2.10}$$

where I_{BT} denotes the boundary term required for a well-defined variational principle.

Taking the first variation and using the Palatini identity, we obtain

$$\begin{aligned} \delta I_R &= \frac{1}{16\pi G}\int d^5x\sqrt{-g}\,(G_{\mu\nu}\,\delta g^{\mu\nu} + g^{\mu\nu}\,\delta R_{\mu\nu}) + \delta I_{BT}, \\ &= \frac{1}{16\pi G}\int d^5x\sqrt{-g}\,(-G^{\mu\nu}\,\delta g_{\mu\nu})\,, \end{aligned} \tag{4.2.11}$$

where in the last step we have used that the boundary term I_{BT} is chosen so as to enforce Dirichlet boundary conditions, thereby cancelling the total-derivative contribution arising from $g^{\mu\nu}\delta R_{\mu\nu}$.

The first functional derivative then follows as

$$\frac{\delta I_R}{\delta g_{\mu\nu}(x)} = -\frac{1}{16\pi G}\sqrt{-g}\, G^{\mu\nu}\Big|_x\,. \tag{4.2.12}$$

At this stage the result is still completely standard: the Einstein tensor controls the linearized response of the action. The genuinely new information needed for the one loop problem enters at the next step, namely the second variation. To obtain the second functional derivative, we vary (4.2.12) once more:

$$
\begin{aligned}
&\delta\left(\frac{\delta I_R}{\delta g_{\mu\nu}(x)}\right) && (4.2.13)\\
&= -\frac{1}{16\pi G}\,\delta\big(\sqrt{-g}\,G^{\mu\nu}\big)\,,\\
&= -\frac{1}{16\pi G}\sqrt{-g}\left(\frac{1}{2}g^{\alpha\beta}\delta g_{\alpha\beta}\,G^{\mu\nu} + \delta g^{\mu\alpha}G_{\alpha}{}^{\nu} + \delta g^{\nu\beta}G^{\mu}{}_{\beta} + g^{\mu\alpha}g^{\nu\beta}\delta G_{\alpha\beta}\right),\\
&= -\frac{1}{16\pi G}\sqrt{-g}\left[\left(\frac{1}{2}g^{\alpha\beta}G^{\mu\nu} - g^{\mu\alpha}g^{\beta\lambda}G_{\lambda}{}^{\nu} - g^{\nu\alpha}g^{\beta\lambda}G^{\mu}{}_{\lambda}\right)\delta g_{\alpha\beta} + g^{\mu\alpha}g^{\nu\beta}\delta G_{\alpha\beta}\right].
\end{aligned}
\tag{4.2.14}
$$

To complete the computation of the second variation, we now derive the explicit expression for $\delta G_{\mu\nu}$, which is the object that carries the differential structure of the quadratic operator. This is the point where the fluctuation problem starts acquiring its characteristic operator form.

The variation of the Christoffel symbols and the Riemann tensor is given by

$$
\delta\Gamma^{\mu}{}_{\rho\sigma} = \frac{1}{2}g^{\mu\lambda}\left(\nabla_\rho\delta g_{\sigma\lambda} + \nabla_\sigma\delta g_{\rho\lambda} - \nabla_\lambda\delta g_{\rho\sigma}\right)\,, \tag{4.2.15}
$$

$$
\delta R^{\mu}{}_{\lambda\rho\sigma} = \nabla_\rho\delta\Gamma^{\mu}{}_{\sigma\lambda} - \nabla_\sigma\delta\Gamma^{\mu}{}_{\rho\lambda}\,. \tag{4.2.16}
$$

From now on, it is convenient to switch from the abstract variation notation to the fluctuation field itself. We therefore define the metric perturbation

$$
h_{\mu\nu} \equiv \delta g_{\mu\nu}\,, \tag{4.2.17}
$$

$$
h \equiv g^{\mu\nu}h_{\mu\nu}\,, \tag{4.2.18}
$$

where $h_{\mu\nu}$ is an arbitrary symmetric tensor. It follows that $\delta g^{\mu\nu} = -h^{\mu\nu}$, and therefore

$$
\delta\Gamma^{\mu}{}_{\rho\sigma} = \frac{1}{2}\left(\nabla_\rho h_\sigma{}^{\mu} + \nabla_\sigma h_\rho{}^{\mu} - \nabla^\mu h_{\rho\sigma}\right)\,, \tag{4.2.19}
$$

$$
\delta\Gamma^{\rho}{}_{\rho\mu} = \frac{1}{2}\nabla_\mu h\,. \tag{4.2.20}
$$

The next step is to express the curvature variations directly in terms of $h_{\mu\nu}$. The variation of the Ricci tensor is then

$$\begin{aligned}\delta R_{\lambda\sigma} &= \nabla_\rho \delta\Gamma^\rho{}_{\sigma\lambda} - \nabla_\sigma \delta\Gamma^\rho{}_{\rho\lambda} \\ &= \frac{1}{2}\left(\nabla_\rho\nabla_\sigma h_\lambda{}^\rho + \nabla_\rho\nabla_\lambda h_\sigma{}^\rho - \nabla_\rho\nabla^\rho h_{\lambda\sigma} - \nabla_\sigma\nabla_\lambda h\right) . \end{aligned} \tag{4.2.21}$$

Taking the trace, we obtain

$$g^{\lambda\sigma}\delta R_{\lambda\sigma} = \nabla_\rho\nabla_\sigma h^{\rho\sigma} - \nabla_\rho\nabla^\rho h\,. \tag{4.2.22}$$

The variation of the Ricci scalar follows as

$$\begin{aligned}\delta R &= \delta g^{\mu\nu} R_{\mu\nu} + g^{\mu\nu}\delta R_{\mu\nu}, \\ &= -h^{\mu\nu}R_{\mu\nu} + \nabla_\rho\nabla_\sigma h^{\rho\sigma} - \nabla_\rho\nabla^\rho h\,. \end{aligned} \tag{4.2.23}$$

Using these results, the variation of the Einstein tensor is

$$\begin{aligned}\delta G_{\mu\nu} &= \delta R_{\mu\nu} - \frac{1}{2}R\,\delta g_{\mu\nu} - \frac{1}{2}g_{\mu\nu}\,\delta R, \\ &= \frac{1}{2}\left(\nabla_\rho\nabla_\mu h_\nu{}^\rho + \nabla_\rho\nabla_\nu h_\mu{}^\rho - \nabla_\rho\nabla^\rho h_{\mu\nu} - \nabla_\mu\nabla_\nu h\right) - \frac{1}{2}R\,h_{\mu\nu} \\ &\quad - \frac{1}{2}g_{\mu\nu}\left(-h^{\rho\sigma}R_{\rho\sigma} + \nabla_\rho\nabla_\sigma h^{\rho\sigma} - \nabla_\rho\nabla^\rho h\right) . \end{aligned} \tag{4.2.24}$$

To make the geometric structure explicit, we commute covariant derivatives. Using

$$\nabla_\rho\nabla_\mu h_\nu{}^\rho = \nabla_\mu\nabla_\rho h_\nu{}^\rho + R_{\nu\lambda\rho\mu}h^{\lambda\rho} + R_{\lambda\mu}h_\nu{}^\lambda\,, \tag{4.2.25}$$

$$\nabla_\rho\nabla_\nu h_\mu{}^\rho = \nabla_\nu\nabla_\rho h_\mu{}^\rho + R_{\mu\lambda\rho\nu}h^{\lambda\rho} + R_{\lambda\nu}h_\mu{}^\lambda\,, \tag{4.2.26}$$

we obtain

$$\begin{aligned}\delta G_{\mu\nu} &= \frac{1}{2}\left(\nabla_\mu\nabla_\rho h_\nu{}^\rho + \nabla_\nu\nabla_\rho h_\mu{}^\rho - \nabla_\rho\nabla^\rho h_{\mu\nu} - \nabla_\mu\nabla_\nu h\right) \\ &\quad + R_{\mu\lambda\nu\rho}h^{\lambda\rho} + \frac{1}{2}\left(R_{\lambda\mu}h_\nu{}^\lambda + R_{\lambda\nu}h_\mu{}^\lambda\right) - \frac{1}{2}R\,h_{\mu\nu} \\ &\quad - \frac{1}{2}g_{\mu\nu}\left(-h^{\rho\sigma}R_{\rho\sigma} + \nabla_\rho\nabla_\sigma h^{\rho\sigma} - \nabla_\rho\nabla^\rho h\right) . \end{aligned} \tag{4.2.27}$$

Thus, the linearised Einstein tensor $\delta G_{\mu\nu}$ evaluated on the perturbation $h_{\mu\nu}$ takes the form

$$\begin{aligned}\delta G_{\mu\nu} &= \frac{1}{2}\nabla_\nu\nabla_\rho h_\mu{}^\rho + \frac{1}{2}\nabla_\mu\nabla_\rho h_\nu{}^\rho + R_{\mu\lambda\rho\nu}h^{\lambda\rho} + \frac{1}{2}R_{\lambda\nu}h_\mu{}^\lambda + \frac{1}{2}R_{\lambda\mu}h_\nu{}^\lambda \\ &\quad - \frac{1}{2}\nabla_\rho\nabla^\rho h_{\mu\nu} - \frac{1}{2}\nabla_\mu\nabla_\nu h - \frac{1}{2}h_{\mu\nu}R \\ &\quad - \frac{1}{2}g_{\mu\nu}(-h^{\rho\sigma}R_{\rho\sigma} + \nabla_\rho\nabla_\sigma h^{\rho\sigma} - \nabla_\rho\nabla^\rho h) \equiv W_{\mu\nu}{}^{\alpha\beta}\,\delta g_{\alpha\beta}\,. \end{aligned} \tag{4.2.28}$$

Substituting (4.2.28) in (4.2.14) and then taking the variation with respect to $\delta g_{\alpha\beta}(y)$, we obtain

$$\frac{\delta^2 I_R}{\delta g_{\alpha\beta}(y)\,\delta g_{\mu\nu}(x)}, \tag{4.2.29}$$

$$= -\frac{1}{16\pi G}\sqrt{-g}\left[\frac{1}{2}g^{\alpha\beta}G^{\mu\nu} - g^{\mu\alpha}g^{\eta\beta}G_\eta{}^\nu - g^{\nu\alpha}g^{\eta\beta}G^\mu{}_\eta + g^{\mu\eta}g^{\nu\xi}W_{\eta\xi}{}^{\alpha\beta}\right]\delta^{(5)}(x-y)\,. \tag{4.2.30}$$

Substituting into the second-order term in the saddle-point expansion, we obtain

$$\begin{aligned} I_R^{(h,h)} &\equiv \frac{1}{2!}\int_M d^5y\,d^5x\,\frac{\delta^2 S}{\delta g_{\alpha\beta}(y)\,\delta g_{\mu\nu}(x)}h_{\alpha\beta}(y)h_{\mu\nu}(x) \\ &= -\frac{1}{32\pi G}\int_M d^5x\sqrt{-g}\left[\frac{1}{2}g^{\alpha\beta}G^{\mu\nu} - 2g^{\mu\alpha}g^{\eta\beta}G_\eta{}^\nu + g^{\mu\eta}g^{\nu\xi}W_{\eta\xi}{}^{\alpha\beta}\right]h_{\alpha\beta}h_{\mu\nu}\,, \end{aligned} \tag{4.2.31}$$

where we used the symmetry of the integrand under the interchange $(\mu\nu) \leftrightarrow (\alpha\beta)$ to combine the two $G_{\mu\nu}$-dependent terms. It remains to evaluate the contraction $W^{\alpha\beta,\mu\nu}h_{\alpha\beta}h_{\mu\nu}$. Expanding explicitly:

$$\begin{aligned} W^{\alpha\beta,\mu\nu}h_{\alpha\beta}h_{\mu\nu} &= h^{\mu\nu}\nabla_\nu\nabla_\rho h_\mu{}^\rho + h^{\mu\nu}R_{\mu\lambda\rho\nu}h^{\lambda\rho} + h^{\mu\nu}R_{\lambda\nu}h_\mu{}^\lambda \\ &\quad - \frac{1}{2}h^{\mu\nu}\nabla_\rho\nabla^\rho h_{\mu\nu} - \frac{1}{2}h^{\mu\nu}\nabla_\mu\nabla_\nu h - \frac{1}{2}h^{\mu\nu}h_{\mu\nu}R \\ &\quad + \frac{1}{2}h\,h^{\rho\sigma}R_{\rho\sigma} - \frac{1}{2}h\,\nabla_\rho\nabla_\sigma h^{\rho\sigma} + \frac{1}{2}h\,\nabla_\rho\nabla^\rho h\,. \end{aligned} \tag{4.2.32}$$

Integrating by parts and discarding total derivatives, the underlined terms combine as follows:

$$W^{\alpha\beta,\mu\nu}h_{\alpha\beta}h_{\mu\nu} = -\nabla_\nu h^{\mu\nu}\nabla_\rho h_\mu{}^\rho + h^{\mu\nu}R_{\mu\lambda\rho\nu}h^{\lambda\rho} + h^{\mu\nu}R_{\lambda\nu}h_\mu{}^\lambda \\ -\frac{1}{2}h^{\mu\nu}\nabla_\rho\nabla^\rho h_{\mu\nu} + \nabla_\mu h^{\mu\nu}\nabla_\nu h - \frac{1}{2}h^{\mu\nu}h_{\mu\nu}R \\ +\frac{1}{2}h\,h^{\rho\sigma}R_{\rho\sigma} - \frac{1}{2}\nabla_\rho h\,\nabla^\rho h + \nabla(\cdots)\,. \tag{4.2.33}$$

To simplify the violet-coloured terms, we introduce the gauge-fixing combination

$$\mathfrak{G} \equiv g^{\mu\nu}\left(\nabla_\rho h_\mu{}^\rho - \frac{1}{2}\nabla_\mu h\right)\left(\nabla_\sigma h_\nu{}^\sigma - \frac{1}{2}\nabla_\nu h\right), \\ = \nabla_\rho h_\mu{}^\rho\nabla_\sigma h^{\mu\sigma} - \nabla_\rho h_\mu{}^\rho\nabla^\mu h + \frac{1}{4}\nabla_\mu h\,\nabla^\mu h\,, \tag{4.2.34}$$

which immediately gives

$$-\nabla_\nu h^{\mu\nu}\nabla_\rho h_\mu{}^\rho + \nabla_\mu h^{\mu\nu}\nabla_\nu h = -\mathfrak{G} + \frac{1}{4}\nabla_\mu h\,\nabla^\mu h\,. \tag{4.2.35}$$

Substituting back and grouping terms by the tensor structures acting on $h_{\alpha\beta}$ from the left and $h_{\mu\nu}$ from the right, we arrive at

$$W^{\alpha\beta,\mu\nu}h_{\alpha\beta}h_{\mu\nu} = h_{\alpha\beta}\left[\frac{1}{4}g^{\alpha\beta}g^{\mu\nu}\Box + R^{\mu\alpha\beta\nu} + g^{\beta\mu}R^{\alpha\nu} - \frac{1}{2}g^{\mu\alpha}g^{\nu\beta}\Box - \frac{1}{2}g^{\mu\alpha}g^{\nu\beta}R \right.\\ \left. +\frac{1}{2}g^{\alpha\beta}R^{\mu\nu}\right]h_{\mu\nu}, \\ = \quad -\mathfrak{G} + \nabla(\cdots)\,. \tag{4.2.36}$$

Inserting this result into (4.2.31) and using the decomposition $G^{\mu\nu} = R^{\mu\nu} - \frac{1}{2}g^{\mu\nu}R$ to rewrite the terms involving the Einstein tensor, we find

$$I_R^{(h,h)} = \frac{1}{16\pi G}\int_M d^5x\sqrt{-g}\,h_{\alpha\beta}\left[\frac{1}{4}g^{\mu\alpha}g^{\nu\beta}\Box - \frac{1}{8}g^{\alpha\beta}g^{\mu\nu}\Box - \frac{1}{2}R^{\mu\alpha\beta\nu} + \frac{1}{2}g^{\beta\mu}R^{\alpha\nu}\right.\\ \left.-\frac{1}{2}g^{\mu\nu}R^{\alpha\beta} - \frac{1}{4}g^{\mu\alpha}g^{\nu\beta}R + \frac{1}{8}Rg^{\alpha\beta}g^{\mu\nu}\right]h_{\mu\nu} \\ +\frac{1}{32\pi G}\int d^5x\sqrt{-g}\,g^{\mu\nu}\left(\nabla_\rho h_\mu{}^\rho - \frac{1}{2}\nabla_\mu h\right)\left(\nabla_\sigma h_\nu{}^\sigma - \frac{1}{2}\nabla_\nu h\right)\,. \tag{4.2.37}$$

This is the standard Lichnerowicz form of the quadratic gravitational action, which will serve as the starting point for the stability analysis in subsequent sections.

4.2.1.2 Cosmological constant sector

We now turn to the contribution arising from the cosmological constant term. In contrast to the Einstein Hilbert sector, this contribution is purely algebraic in the metric and does not involve derivatives, which considerably simplifies its second variation.

The variation of the first functional derivative of I_Λ with respect to the metric yields

$$\delta\left(\frac{\delta I_\Lambda}{\delta g_{\mu\nu}(x)}\right) = -\frac{\sqrt{-g}\,\Lambda}{\kappa^2}\left(\frac{1}{2}g^{\rho\sigma}\delta g_{\rho\sigma}\,g^{\mu\nu} - g^{\rho\mu}g^{\sigma\nu}\delta g_{\rho\sigma}\right) . \tag{4.2.38}$$

From this expression, the second functional derivative follows as

$$\frac{\delta^2 I_\Lambda}{\delta g_{\rho\sigma}(y)\,\delta g_{\mu\nu}(x)} = -\frac{\sqrt{-g}\,\Lambda}{\kappa^2}\,\delta^{(5)}(x-y)\left(\frac{1}{2}g^{\rho\sigma}g^{\mu\nu} - g^{\mu(\rho}g^{\sigma)\nu}\right) . \tag{4.2.39}$$

Substituting into the definition of $I_\Lambda^{(h,h)}$, we obtain the quadratic contribution

$$I_\Lambda^{(h,h)} = \frac{1}{\kappa^2}\int d^5x\sqrt{-g}\,h_{\rho\sigma}\left(-\frac{\Lambda}{4}g^{\rho\sigma}g^{\mu\nu} + \frac{\Lambda}{2}g^{\mu\rho}g^{\sigma\nu}\right)h_{\mu\nu} . \tag{4.2.40}$$

This contribution acts as an effective mass-like term for the metric perturbations, in contrast to the kinetic structure arising from the Einstein Hilbert sector. In the following, we proceed to analyze the remaining contributions to the quadratic action.

4.2.1.3 Gauge field sector

We now compute the contribution to the quadratic action arising from the gauge-field sector due to metric fluctuations. This requires evaluating the second functional derivative of $I_A[g, A]$ with respect to the metric.

We begin by varying the first functional derivative,

$$\delta_g\left(\frac{\delta I_A}{\delta g_{\mu\nu}(x)}\right) = \delta_g\left[\frac{2\sqrt{-g}}{\kappa^2}\left(F^\mu{}_\rho F^{\nu\rho} - \frac{1}{4}g^{\mu\nu}F_{\rho\sigma}F^{\rho\sigma}\right)\right] . \tag{4.2.41}$$

Performing the variation, and using $\delta g^{\mu\nu} = -h^{\mu\nu}$, we obtain

$$\delta_g \left(\frac{\delta I_A}{\delta g_{\mu\nu}(x)} \right) = \frac{2\sqrt{-g}}{\kappa^2} \Bigg[\frac{1}{2} g^{\rho\sigma} \delta g_{\rho\sigma} T^{\mu\nu} - \delta g_{\rho\sigma} g^{\mu\rho} F^{\sigma\lambda} F^{\nu}{}_{\lambda} - \delta g_{\rho\sigma} g^{\nu\rho} F^{\mu}{}_{\lambda} F^{\sigma\lambda} \\ - \delta g_{\rho\sigma} F^{\mu\rho} F^{\nu\sigma} + \frac{1}{4} \delta g_{\rho\sigma} g^{\rho\mu} g^{\sigma\nu} F_{\alpha\beta} F^{\alpha\beta} + \frac{1}{2} g^{\mu\nu} \delta g_{\rho\sigma} F^{\rho}{}_{\lambda} F^{\sigma\lambda} \Bigg] . \tag{4.2.42}$$

From this, the second functional derivative follows as

$$\frac{\delta^2 I_A}{\delta g_{\rho\sigma}(y) \delta g_{\mu\nu}(x)} = \frac{2\sqrt{-g}}{\kappa^2} \delta^{(5)}(x-y) \Bigg[\frac{1}{2} g^{\rho\sigma} T^{\mu\nu} - g^{\mu(\rho} F^{\sigma)\lambda} F^{\nu}{}_{\lambda} - g^{\nu(\rho} F^{\sigma)\lambda} F^{\mu}{}_{\lambda} \\ - F^{\mu(\rho} F^{\nu\sigma)} + \frac{1}{4} g^{\mu(\rho} g^{\sigma)\nu} F_{\alpha\beta} F^{\alpha\beta} + \frac{1}{2} g^{\mu\nu} F^{(\rho}{}_{\lambda} F^{\sigma)\lambda} \Bigg] . \tag{4.2.43}$$

Substituting into the definition of $I_A^{(h,h)}$, we obtain

$$I_A^{(h,h)} = \frac{1}{\kappa^2} \int d^5x \sqrt{-g}\, h_{\rho\sigma} \Bigg[\frac{1}{2} g^{\rho\sigma} T^{\mu\nu} - g^{\mu\rho} F^{\sigma\lambda} F^{\nu}{}_{\lambda} - g^{\nu\rho} F^{\mu}{}_{\lambda} F^{\sigma\lambda} \\ - F^{\mu\rho} F^{\nu\sigma} + \frac{1}{4} g^{\mu\rho} g^{\sigma\nu} F_{\alpha\beta} F^{\alpha\beta} + \frac{1}{2} g^{\mu\nu} F^{\rho}{}_{\lambda} F^{\sigma\lambda} \Bigg] h_{\mu\nu} . \tag{4.2.44}$$

Replacing $T^{\mu\nu}$, the expression simplifies to

$$I_A^{(h,h)} = \frac{1}{\kappa^2} \int d^5x \sqrt{-g}\, h_{\rho\sigma} \Bigg[\frac{1}{8} F_{\alpha\beta} F^{\alpha\beta} \left(2 g^{\rho\mu} g^{\sigma\nu} - g^{\rho\sigma} g^{\mu\nu} \right) - F^{\mu\rho} F^{\nu\sigma} \\ - 2 F^{\rho\lambda} F^{\mu}{}_{\lambda} g^{\sigma\nu} + g^{\mu\nu} F^{\rho}{}_{\lambda} F^{\sigma\lambda} \Bigg] h_{\mu\nu} . \tag{4.2.45}$$

Finally, exploiting the symmetry under the interchange $(\mu\nu) \leftrightarrow (\rho\sigma)$, the expression can be written in the manifestly symmetric form above.

4.2.1.4 Gauss-Bonnet sector

We now turn to the Gauss-Bonnet contribution, which constitutes the most intricate part of the quadratic expansion. While its structure is analogous to that of the Einstein Hilbert sector, it involves the variation of the Lanczos-Lovelock tensor $H_{\mu\nu}$, whose dependence on curvature tensors leads to a significantly more intricate tensorial structure.

Starting from the first functional derivative, the second variation reads

$$\delta\left(\frac{\delta I_{\mathcal{G}}}{\delta g_{\mu\nu}(x)}\right) = -\frac{\alpha\sqrt{-g}}{2\kappa^2}\left(\frac{1}{2}g^{\rho\sigma}\delta g_{\rho\sigma}\, H^{\mu\nu} - \delta g_{\rho\sigma}\, g^{\mu\rho}H^{\sigma\nu} - \delta g_{\rho\sigma}\, g^{\nu\rho}H^{\mu\sigma} + g^{\mu\lambda}g^{\nu\delta}\,\delta H_{\lambda\delta}\right). \tag{4.2.46}$$

The first three terms are purely algebraic in the metric perturbation, while the last term encodes the non-trivial differential structure through the variation of $H_{\mu\nu}$. To make this structure explicit, we introduce the linear operator

$$\delta H_{\mu\nu} \equiv \mathsf{P}[H]_{\mu\nu}{}^{\rho\sigma}\, h_{\rho\sigma}\,, \tag{4.2.47}$$

where $\mathsf{P}[H]$ is a second-order differential operator acting on symmetric tensors.

With this definition, the second functional derivative can be written compactly as

$$\frac{\delta^2 I_{\mathcal{G}}}{\delta g_{\rho\sigma}(y)\,\delta g_{\mu\nu}(x)} = -\frac{\alpha\sqrt{-g}}{2\kappa^2}\,\delta^{(5)}(x-y)\left(\frac{1}{2}g^{\rho\sigma}H^{\mu\nu} - g^{\mu(\rho}H^{\sigma)\nu} - g^{\nu(\rho}H^{\sigma)\mu} + \mathsf{P}[H]^{\mu\nu,\rho\sigma}\right). \tag{4.2.48}$$

Substituting into the quadratic form, we obtain

$$I_{\mathcal{G}}^{(h,h)} = \frac{1}{\kappa^2}\int d^5x\sqrt{-g}\, h_{\mu\nu}\left(-\frac{\alpha}{4}g^{\rho\sigma}H^{\mu\nu} + \alpha g^{\mu\rho}H^{\sigma\nu} - \frac{\alpha}{2}\mathsf{P}[H]^{\mu\nu,\rho\sigma}\right)h_{\rho\sigma}\,. \tag{4.2.49}$$

To determine the explicit form of $\mathsf{P}[H]$, we compute the variation of the Lanczos-Lovelock tensor term by term. Conceptually, this is the analogue of the Einstein Hilbert computation performed above, but with a much more elaborate tensorial structure. Recall that

$$H_{\mu\nu} = 2RR_{\mu\nu} - 4R_{\mu\rho}R^{\rho}{}_{\nu} - 4R^{\delta}{}_{\rho}R^{\rho}{}_{\mu\delta\nu} + 2R_{\mu\rho\sigma\delta}R_{\nu}{}^{\rho\sigma\delta} - \frac{1}{2}\mathcal{G}\, g_{\mu\nu}\,, \tag{4.2.50}$$

which we decompose as $H_{\mu\nu} = \sum_{i=1}^{5}\mathsf{t}^{(i)}_{\mu\nu}$, where $\mathsf{t}^{(i)}_{\mu\nu}$ is the i-th term in the Eq.(4.2.50).

The variation is therefore

$$\delta H_{\mu\nu} = \sum_{i=1}^{5} \delta \mathsf{t}^{(i)}_{\mu\nu} \,, \tag{4.2.51}$$

and each contribution can be computed using the standard first-order variations of the curvature tensors.

The explicit expressions for $\delta\mathsf{t}^{(i)}_{\mu\nu}$ are obtained by straightforward, albeit lengthy, substitutions of the identities for δR, $\delta R_{\mu\nu}$, and $\delta R_{\mu\nu\rho\sigma}$. For completeness, we list the resulting contributions. The important point to keep in mind is that, despite their complexity, all of them fit into the same general pattern: algebraic curvature couplings plus a second-order differential action on $h_{\mu\nu}$.

Collecting all terms, the operator $\mathsf{P}[H]$ is defined implicitly through

$$h^{\mu\nu}\, \mathsf{P}[H]_{\mu\nu}{}^{\rho\sigma} h_{\rho\sigma} = h^{\mu\nu}\, \delta H_{\mu\nu} = h^{\mu\nu} \sum_{i=1}^{5} \delta \mathsf{t}^{(i)}_{\mu\nu} \,, \tag{4.2.52}$$

and can be compactly presented as

$$\begin{aligned}
&g_{\mu\lambda} g_{\nu\delta} \mathsf{P}^{\lambda\delta,\rho\sigma} h_{\rho\sigma} = \\
&-\frac{1}{2} h_{\mu\nu}\mathcal{G} - h^{\gamma\delta}\left[2R_{\gamma\delta}R_{\mu\nu} - 4R_{\mu\gamma}R_{\nu\delta} - 4R_{\gamma\eta\delta\lambda}R_{\mu}{}^{\eta}{}_{\nu}{}^{\lambda} + R_{\mu\gamma\eta\lambda}R_{\nu\delta}{}^{\eta\lambda} + 2R_{\mu}{}^{\eta}{}_{\gamma}{}^{\lambda}R_{\nu\lambda\delta\eta}\right. \\
&\left.+R_{\mu\gamma}{}^{\eta\lambda}(R_{\nu\delta\eta\lambda} - 2R_{\nu\eta\delta\lambda}) + 2R_{\mu\eta\gamma\lambda}(-R_{\nu\delta}{}^{\eta\lambda} + R_{\nu}{}^{\lambda}{}_{\delta}{}^{\eta})\right] + R_{\mu\nu}(\nabla_\delta\nabla_\gamma h^{\gamma\delta} - \Box h) \\
&+ 4R_{(\mu|}{}^{\gamma}\left[\nabla_\gamma\nabla_{|\nu)}h - \nabla_\delta\nabla_\gamma h_{|\nu)}{}^{\delta} + \Box h_{|\nu)\gamma} - \nabla_\delta\nabla_{|\nu)}h_\gamma{}^{\delta}\right] + 2R_{\mu\gamma\nu\delta}\Box h^{\gamma\delta} - 2R_{\nu\eta\gamma\delta}\nabla^\eta\nabla^\delta h_\mu{}^\gamma \\
&- (R_{\mu\delta\nu\eta} + R_{\mu\eta\nu\delta})(2\nabla^\eta\nabla_\gamma h^{\gamma\delta} - \nabla^\eta\nabla^\delta h) - 2R_{\mu\eta\gamma\delta}\nabla^\eta\nabla^\delta h_\nu{}^\gamma + 2R_{\nu\gamma\delta\eta}\nabla^\eta\nabla_\mu h^{\gamma\delta} \\
&+ 2R_{\mu\gamma\delta\eta}\nabla^\eta\nabla_\nu h^{\gamma\delta} + g_{\mu\nu}\left[h^{\gamma\delta}(-4R_\gamma{}^\eta R_{\delta\eta} + R_{\gamma\delta}R + R_\gamma{}^{\eta\lambda\xi}R_{\delta\eta\lambda\xi}) - R\nabla_\delta\nabla_\gamma h^{\gamma\delta}\right. \\
&\left.+R\Box h - 2R^{\gamma\delta}\left(\nabla_\delta\nabla_\gamma h - 2\nabla_\eta\nabla_\delta h_\gamma{}^\eta + \Box h_{\gamma\delta}\right) + 2R_{\gamma\eta\delta\lambda}\nabla^\lambda\nabla^\eta h^{\gamma\delta}\right] \\
&+ R^{\gamma\delta}\left(2\nabla_\delta\nabla_\gamma h_{\mu\nu} - 2\nabla_\delta\nabla_\mu h_{\nu\gamma} - 2\nabla_\delta\nabla_\nu h_{\mu\gamma} + \nabla_\mu\nabla_\nu h_{\gamma\delta} + \nabla_\nu\nabla_\mu h_{\gamma\delta}\right) \\
&- \frac{1}{2}R\left(2\Box h_{\mu\nu} - 2\nabla_\gamma\nabla_\mu h_\nu{}^\gamma - 2\nabla_\gamma\nabla_\nu h_\mu{}^\gamma + \nabla_\mu\nabla_\nu h + \nabla_\nu\nabla_\mu h\right)\,.
\end{aligned} \tag{4.2.53}$$

Finally, the quadratic contribution from the Gauss-Bonnet sector is fully determined by substituting this result into (4.2.49).

4.2.2 Computation of interaction terms $I^{(h,a)}$ and $I^{(a,h)}$

Before turning to the individual contributions, let us make explicit the general step that will be used repeatedly below. Suppose that, after varying a first functional derivative of the action with respect to a fluctuation field $\varphi(y)$, one obtains a local expression of the form

$$\delta_\varphi\left(\frac{\delta I}{\delta\Phi(x)}\right) = \mathcal{L}(x;\varphi), \tag{4.2.54}$$

where $\mathcal{L}(x;\varphi)$ depends only on $\varphi(x)$ and its derivatives evaluated at the same spacetime point x. By definition of the second functional derivative,

$$\delta_\varphi\left(\frac{\delta I}{\delta\Phi(x)}\right) = \int d^5y\,\varphi(y)\,\frac{\delta^2 I}{\delta\varphi(y)\,\delta\Phi(x)}. \tag{4.2.55}$$

Since the left-hand side of Eq. (4.2.54) is local in x, the second functional derivative must have support only at $x=y$, and therefore it is proportional to $\delta^{(5)}(x-y)$. Substituting this into a quadratic term of the form

$$I^{(2)} = \frac{1}{2}\int d^5x \int d^5y\,\varphi(y)\,\frac{\delta^2 I}{\delta\varphi(y)\,\delta\Phi(x)}\,\chi(x), \tag{4.2.56}$$

the integration over y immediately collapses and one obtains a single spacetime integral. In what follows, we shall only display the explicit local variations and the resulting quadratic expressions.

We first compute $I_A^{(h,a)}$. Starting from the first functional derivative of the Maxwell sector with respect to the gauge field,

$$\frac{\delta I_A}{\delta A_\mu(x)} = \frac{4\sqrt{-g}}{\kappa^2}\nabla_\rho F^{\rho\mu} = \frac{4}{\kappa^2}\partial_\rho\big(\sqrt{-g}\,F^{\rho\mu}\big), \tag{4.2.57}$$

variation with respect to the metric perturbation gives

$$\begin{aligned}
\delta_g\left(\frac{\delta I_A}{\delta A_\mu(x)}\right) &= \frac{4}{\kappa^2}\partial_\rho\left[\sqrt{-g}\left(\frac{1}{2}g^{\lambda\sigma}h_{\lambda\sigma}F^{\rho\mu} - h^{\rho\lambda}F_\lambda{}^\mu - h^{\mu\lambda}F^\rho{}_\lambda\right)\right], \\
&= \frac{4}{\kappa^2}\partial_\rho\left[\sqrt{-g}\left(\frac{1}{2}g^{\lambda\sigma}h_{\lambda\sigma}F^{\rho\mu} - 2h^{\lambda[\rho}F_\lambda{}^{\mu]}\right)\right], \\
&= \frac{4\sqrt{-g}}{\kappa^2}\nabla_\rho\left(\frac{1}{2}g^{\lambda\sigma}h_{\lambda\sigma}F^{\rho\mu} - 2h^{\lambda[\rho}F_\lambda{}^{\mu]}\right).
\end{aligned}$$

Therefore,

$$\delta_g\left(\frac{\delta I_A}{\delta A_\mu(x)}\right)=\frac{4\sqrt{-g}}{\kappa^2}\left(\frac{1}{2}\nabla_\rho h_\lambda{}^\lambda\, F^{\rho\mu}+\frac{1}{2}h_\lambda{}^\lambda\,\nabla_\rho F^{\rho\mu}-2\nabla_\rho h^{\lambda[\rho}F_\lambda{}^{\mu]}-2h^{\lambda[\rho}\nabla_\rho F_\lambda{}^{\mu]}\right). \tag{4.2.58}$$

Using the general procedure explained above, Eq. (4.2.58) immediately determines the mixed quadratic contribution. Substituting the corresponding local second functional derivative into the mixed term of Eq. (4.1.3), the Dirac delta collapses the y-integration and one obtains

$$I_A^{(h,a)}=\frac{2}{\kappa^2}\int d^5x\sqrt{-g}\Big[\frac{1}{2}(\nabla_\rho h)a_\mu F^{\rho\mu}+\frac{1}{2}h\,a_\mu\nabla_\rho F^{\rho\mu}-2(\nabla_\rho h^{\lambda[\rho})F_\lambda{}^{\mu]}a_\mu \\ -2h^{\lambda[\rho}(\nabla_\rho F_\lambda{}^{\mu]})a_\mu\Big], \tag{4.2.59}$$

where $h\equiv h_\lambda{}^\lambda$.

We now simplify Eq. (4.2.59) by integrating by parts the terms containing derivatives of h. For the trace contribution one finds, up to boundary terms,

$$\frac{1}{2}\int d^5x\sqrt{-g}\,(\nabla_\rho h)F^{\rho\mu}a_\mu=-\frac{1}{2}\int d^5x\sqrt{-g}\,h\left[(\nabla_\rho F^{\rho\mu})a_\mu+F^{\rho\mu}\nabla_\rho a_\mu\right]. \tag{4.2.60}$$

Using Eq. (4.2.60) in Eq. (4.2.59), the terms proportional to $\nabla_\rho F^{\rho\mu}$ cancel and the trace contribution becomes

$$-\frac{1}{2}\int d^5x\sqrt{-g}\,h\,F^{\rho\mu}\nabla_\rho a_\mu. \tag{4.2.61}$$

For the traceless part, integration by parts gives

$$-2\int d^5x\sqrt{-g}\,(\nabla_\rho h^{\lambda[\rho})F_\lambda{}^{\mu]}a_\mu=2\int d^5x\sqrt{-g}\,h^{\lambda[\rho}\left[(\nabla_\rho F_\lambda{}^{\mu]})a_\mu+F_\lambda{}^{\mu]}\nabla_\rho a_\mu\right]. \tag{4.2.62}$$

Replacing Eq. (4.2.62) into Eq. (4.2.59), the terms proportional to $\nabla_\rho F_\lambda{}^\mu$ cancel as well. Combining the resulting expression with Eq. (4.2.61), and rewriting everything in terms of $h_{\alpha\beta}$, we arrive to

$$I_A^{(h,a)}=\frac{1}{\kappa^2}\int d^5x\sqrt{-g}\,h_{\alpha\beta}\left(-g^{\alpha\beta}F^{\mu\nu}-4g^{\alpha\lambda}g^{\beta[\mu}F_\lambda{}^{\nu]}\right)\nabla_\mu a_\nu. \tag{4.2.63}$$

We now turn to $I_A^{(a,h)}$. Starting from the remaining mixed term in Eq. (4.1.3),

$$I_A^{(a,h)} = \frac{1}{2}\int d^5x \int d^5y\, a_\mu(y) \frac{\delta^2 I_A}{\delta A_\mu(y)\,\delta g_{\rho\sigma}(x)} h_{\rho\sigma}(x). \tag{4.2.64}$$

we begin from the first functional derivative of the Maxwell action with respect to the metric,

$$\frac{\delta I_A}{\delta g_{\mu\nu}(x)} = \frac{\sqrt{-g}}{\kappa^2}\left(-\frac{1}{2}g^{\mu\nu}F_{\lambda\delta}F^{\lambda\delta} + 2F^\mu{}_\lambda F^{\nu\lambda}\right). \tag{4.2.65}$$

Using

$$\delta_A F_{\lambda\delta} = 2\nabla_{[\lambda}a_{\delta]}, \tag{4.2.66}$$

one finds

$$\delta_A\left(\frac{\delta I_A}{\delta g_{\mu\nu}(x)}\right) = \frac{2\sqrt{-g}}{\kappa^2}\left[-g^{\mu\nu}F^{\lambda\sigma}\nabla_\lambda a_\sigma + 2(\nabla^\lambda a^{(\mu})F^{\nu)}{}_\lambda - 2F^{(\nu}{}_\lambda\nabla^{\mu)}a^\lambda\right]. \tag{4.2.67}$$

It is convenient to rewrite this expression only after contraction with the symmetric fluctuation $h_{\mu\nu}$:

$$h_{\mu\nu}\,\delta_A\left(\frac{\delta I_A}{\delta g_{\mu\nu}(x)}\right) = \frac{2\sqrt{-g}}{\kappa^2}\,h_{\mu\nu}\left(4g^{\mu[\sigma}F^{\lambda]\nu} - g^{\mu\nu}F^{\lambda\sigma}\right)\nabla_\lambda a_\sigma. \tag{4.2.68}$$

Applying the same argument as above, the corresponding second functional derivative is local. Substituting it into Eq. (4.2.64), the integration over y is immediate and yields

$$I_A^{(a,h)} = \frac{1}{\kappa^2}\int d^5x\sqrt{-g}\,h_{\alpha\beta}\left(-g^{\alpha\beta}F^{\mu\nu} - 4g^{\alpha\lambda}g^{\beta[\mu}F_\lambda{}^{\nu]}\right)\nabla_\mu a_\nu. \tag{4.2.69}$$

Therefore, up to boundary terms we have that

$$I_A^{(a,h)} = I_A^{(h,a)}. \tag{4.2.70}$$

As expected, both terms represent the same mixed quadratic coupling and differ only by the order of functional differentiation.

4.2.3 Computation of $I^{(a,a)}$

We now compute the purely Maxwell contribution $I_A^{(a,a)}$. Starting again from Eq. (4.2.57),

$$\frac{\delta I_A}{\delta A_\mu(x)} = \frac{4\sqrt{-g}}{\kappa^2}\nabla_\rho F^{\rho\mu}. \tag{4.2.71}$$

Varying with respect to the gauge field fluctuation a_ν, and using $\delta_A F^{\rho\mu} = \nabla^\rho a^\mu - \nabla^\mu a^\rho$, one finds,

$$\delta_A\left(\frac{\delta I_A}{\delta A_\mu(x)}\right) = \frac{4\sqrt{-g}}{\kappa^2}\left(\nabla_\rho\nabla^\rho a^\mu - \nabla_\rho\nabla^\mu a^\rho\right). \tag{4.2.72}$$

Applying the same procedure to the purely gauge-field term in Eq. (4.1.3), the corresponding second functional derivative is again local. Substituting it into the quadratic expansion and performing the y-integration gives

$$I_A^{(a,a)} = \frac{2}{\kappa^2}\int d^5x\sqrt{-g}\, a_\mu\left(\nabla_\rho\nabla^\rho a^\mu - \nabla_\rho\nabla^\mu a^\rho\right). \tag{4.2.73}$$

To simplify Eq. (4.2.73), we commute the covariant derivatives in the second term. Using the Ricci identity,

$$\nabla_\rho\nabla^\mu a^\rho = \nabla^\mu\nabla_\rho a^\rho + R^\mu{}_\lambda a^\lambda, \tag{4.2.74}$$

Eq. (4.2.73) becomes

$$I_A^{(a,a)} = \frac{2}{\kappa^2}\int d^5x\sqrt{-g}\left[a_\mu\nabla_\rho\nabla^\rho a^\mu - a_\mu\nabla^\mu\nabla_\rho a^\rho - a_\mu R^\mu{}_\lambda a^\lambda\right]. \tag{4.2.75}$$

It is then convenient to integrate by parts the second term. Discarding boundary terms, one obtains

$$-\int d^5x\sqrt{-g}\, a_\mu\nabla^\mu\nabla_\rho a^\rho = \int d^5x\sqrt{-g}\,(\nabla_\mu a^\mu)^2. \tag{4.2.76}$$

Using Eq. (4.2.76) in Eq. (4.2.75), the quadratic Maxwell contribution can be written as

$$I_A^{(a,a)} = \frac{2}{\kappa^2}\int d^5x\sqrt{-g}\left[a_\mu(\Box g^{\mu\lambda} - R^{\mu\lambda})a_\lambda + (\nabla_\mu a^\mu)^2\right], \tag{4.2.77}$$

where $\Box \equiv \nabla_\rho \nabla^\rho$.

4.3 One-loop partition function and the eigenvalue equation

With the second-order expansion of the action at hand, the quantum corrections to the partition function are encoded in the Euclidean functional integral. After Wick rotating to the Euclidean background metric $\bar{g}_{\mu\nu}$, the semiclassical partition function takes the form

$$Z = e^{-I[\bar{\Phi}]} \int D\phi \, \exp\left(- \int d^5x \sqrt{g}\, \phi^* \mathbb{O} \phi \right) . \tag{4.3.1}$$

If we define the inner product as

$$(\psi, \phi) := \int d^5x \sqrt{g}\, \psi^* \phi \, , \tag{4.3.2}$$

and assume that the operator $\mathbb{O}$ is self-adjoint with respect to this inner product and has a discrete spectrum with a complete set of normalizable orthonormal eigenfunctions $\{u_i\}$ satisfying

$$\mathbb{O} u_i = \lambda_i u_i \, , \qquad (u_i, u_j) = \delta_{ij} \, . \tag{4.3.3}$$

Any fluctuation can be expanded as

$$\phi(x) = \sum_i c_i u_i(x) \, , \tag{4.3.4}$$

with complex coefficients c_i. Using orthonormality, the quadratic form diagonalizes as

$$(\phi, \mathbb{O}\phi) = \sum_i \lambda_i |c_i|^2 \, . \tag{4.3.5}$$

The functional measure is defined by projecting onto this basis, as the same way as we did in section 2.2 for the harmonic oscillator,

$$D\phi = \prod_i dc_i \, dc_i^* \, , \tag{4.3.6}$$

up to an overall normalization constant. Therefore, the functional integral factorizes into an infinite product of Gaussian integrals,

$$Z_{\text{1-loop}} = \int D\phi \, e^{-(\phi, \mathbb{O}\phi)} \, . \tag{4.3.7}$$

For the bosonic fluctuations considered here, the resulting Gaussian integration yields the usual square-root dependence on the determinant, namely

$$Z_{\text{1-loop}} \propto (\det \mathbb{O})^{-1/2} \, . \tag{4.3.8}$$

Absorbing the field-independent normalization constant into the definition of the path integral, one obtains

$$Z \sim e^{-I[\bar{\Phi}]} \frac{1}{\sqrt{\det \mathbb{O}}} = e^{-I[\bar{\Phi}]} \prod_i \frac{1}{\sqrt{\lambda_i}} \, . \tag{4.3.9}$$

Although we have focused on bosonic fields, gauge invariance requires the inclusion of Faddeev-Popov ghosts associated with diffeomorphism and $U(1)$ symmetries.

A crucial subtlety arises from the presence of zero modes of $\mathbb{O}$, which render the determinant ill-defined and require a suitable regularization. As will be discussed below, these zero modes are precisely responsible for the logarithmic corrections to the entropy.

This mechanism can be understood by viewing the near-extremal, near-horizon geometry (3.3.3) as a deformation of the $\text{AdS}_2 \times S^3$ background, with the deviation controlled linearly by the temperature T. Accordingly, the operator $\mathbb{O}$ admits a decomposition of the form

$$\mathbb{O} = \mathbb{O}_{\text{AdS}_2 \times S^3} + \delta\mathbb{O} \, , \tag{4.3.10}$$

where $\delta\mathbb{O}$ is linear in T.

Let $\{u_i\}$ denote the orthonormal eigenfunctions of the unperturbed operator $\mathbb{O}_{\text{AdS}_2 \times S^3}$,

$$\mathbb{O}_{\text{AdS}_2 \times S^3} u_i = \lambda_i^{\text{AdS}_2 \times S^3} u_i \, . \tag{4.3.11}$$

Then, at first order in perturbation theory, the eigenvalues of $\mathbb{O}$ are given by

$$\lambda_i = \lambda_i^{\mathrm{AdS}_2 \times S^3} + \delta\lambda_i \,, \tag{4.3.12}$$

with

$$\delta\lambda_i = (u_i, \delta\mathbb{O}\, u_i) \,. \tag{4.3.13}$$

For modes that are non-vanishing in the extremal limit, $\lambda_i^{\mathrm{AdS}_2 \times S^3} \neq 0$, the correction $\delta\lambda_i$ produces only subleading effects in the determinant. However, for zero modes satisfying

$$\lambda_i^{\mathrm{AdS}_2 \times S^3} = 0 \,, \tag{4.3.14}$$

the leading contribution to the eigenvalue arises entirely from the perturbation,

$$\lambda_i \sim \delta\lambda_i \propto T \,. \tag{4.3.15}$$

As a result, the contribution of these modes to the one loop determinant behaves as

$$\prod_{\text{zero modes}} \lambda_i \sim T^{N_0} \,, \tag{4.3.16}$$

where N_0 is the number of zero modes. Taking the logarithm, this produces a term proportional to

$$\log Z_{\text{1-loop}} \supset -\frac{N_0}{2} \log\left(\frac{T}{T_0}\right) \,. \tag{4.3.17}$$

which gives rise to logarithmic corrections to the entropy. Here T_0 is an arbitrary reference scale with dimensions of temperature, introduced so that the logarithm has a dimensionless argument. Hence, it follows from (4.3.9) that the logarithmic contribution to the one loop partition function arises exclusively from the zero modes of the $\mathrm{AdS}_2 \times S^3$ background. Indeed,

$$\log Z_{\text{1-loop}} \sim -\frac{1}{2} \sum_i \log\left(\lambda_i^{\mathrm{AdS}_2 \times S^3} + \delta\lambda_i\right) \sim -\frac{1}{2} \sum_i^{(0)} \log(\delta\lambda_i) \,, \tag{4.3.18}$$

where $\sum_i^{(0)}$ denotes the sum over zero modes of $\mathbb{O}_{\mathrm{AdS}_2 \times S^3}$ (see [34–43]).

Therefore, the computation of logarithmic corrections to the entropy reduces to determining the temperature-dependent shift $\delta\lambda_i$ of these zero modes. In what follows, we carry out this computation. Notice that both $\mathbb{O}_{\mathrm{AdS}_2 \times S^3}$ and $\delta\mathbb{O}$ depend non-trivially on the Gauss Bonnet coupling α, as shown in the previous section.

The quadratic operator appearing in (4.3.1) takes the form

$$-\int d^5x\sqrt{g}\,\phi^*\mathbb{O}\phi = -\int d^5x\sqrt{g}\Big[h_{\mu\nu}\mathsf{D}^{\mu\nu,\rho\sigma}h_{\rho\sigma} + h_{\mu\nu}\mathsf{D}^{\mu\nu,\rho}a_\rho + a_\mu\mathsf{D}^{\mu,\rho\sigma}h_{\rho\sigma} + a_\mu\mathsf{D}^{\mu,\rho}a_\rho\Big]\,. \tag{4.3.19}$$

Under the imposed boundary conditions, the mixed terms satisfy

$$h_{\mu\nu}\mathsf{D}^{\mu\nu,\rho}a_\rho = a_\mu\mathsf{D}^{\mu,\rho\sigma}h_{\rho\sigma}\,, \tag{4.3.20}$$

so that the operator is symmetric in the space of fluctuations.

The purely gravitational sector is governed by

$$\begin{aligned} h_{\mu\nu}\mathsf{D}^{\mu\nu,\rho\sigma}h_{\rho\sigma} = -\frac{1}{\kappa^2}h_{\rho\sigma}\Big[&\frac{1}{4}g^{\mu\rho}g^{\nu\sigma}\Box - \frac{1}{8}g^{\rho\sigma}g^{\mu\nu}\Box - \frac{1}{2}R^{\mu\rho\sigma\nu} + \frac{1}{2}g^{\sigma\mu}R^{\rho\nu}\\ &- \frac{1}{2}g^{\mu\nu}R^{\rho\sigma} - \frac{1}{4}g^{\mu\rho}g^{\nu\sigma}R + \frac{1}{8}Rg^{\rho\sigma}g^{\mu\nu}\\ &- \frac{\Lambda}{4}g^{\rho\sigma}g^{\mu\nu} + \frac{\Lambda}{2}g^{\mu\rho}g^{\sigma\nu}\\ &+ \frac{1}{8}F_{\lambda\delta}F^{\lambda\delta}\left(2g^{\rho\mu}g^{\sigma\nu} - g^{\rho\sigma}g^{\mu\nu}\right) - F^{\mu\rho}F^{\nu\sigma}\\ &- 2F^{\rho\lambda}F^{\mu}{}_{\lambda}g^{\sigma\nu} + g^{\mu\nu}F^{\rho}{}_{\lambda}F^{\sigma\lambda}\\ &- \frac{\alpha}{4}g^{\rho\sigma}H^{\mu\nu} + \alpha g^{\mu\rho}H^{\sigma\nu} - \frac{\alpha}{2}\mathsf{P}[H]^{\mu\nu,\rho\sigma}\Big]h_{\mu\nu}\,. \end{aligned} \tag{4.3.21}$$

Finally, the mixed and gauge-field sectors are given by

$$h_{\mu\nu}\mathsf{D}^{\mu\nu,\rho}a_\rho = \frac{2}{\kappa^2}h_{\mu\nu}\left(g^{\mu\nu}F^{\alpha\beta} + 4g^{\mu\lambda}g^{\nu[\alpha}F_{\lambda}{}^{\beta]}\right)\nabla_\alpha a_\beta, \tag{4.3.22}$$

$$a_\mu\mathsf{D}^{\mu,\rho}a_\rho = -\frac{2}{\kappa^2}a_\mu\left(g^{\mu\lambda}\Box - R^{\mu\lambda}\right)a_\lambda. \tag{4.3.23}$$

4.4 Zero Modes

The computation of zero modes arising from the gravitational sector proceeds by exploiting the gauge symmetries of the theory. As in General Relativity, Einstein-Gauss-Bonnet theory is invariant under diffeomorphisms. At the perturbative level, this symmetry acts on the metric fluctuation $h_{\mu\nu}$ around a background $\bar{g}_{\mu\nu}$

through the Lie derivative,

$$\delta_\xi h_{\mu\nu} = \mathcal{L}_\xi \bar{g}_{\mu\nu} \,, \tag{4.4.1}$$

where ξ^μ is a vector field on $\mathcal{M}$.

It is important to note that no ambiguity arises in the number of propagating degrees of freedom, since the Gauss-Bonnet coupling α can be considereda perturbative parameter, and therefore does not introduce additional dynamical modes beyond those of General Relativity [13].

Upon imposing a suitable gauge-fixing condition, zero modes of the operator $\mathbb{O}$ on the extremal near-horizon geometry can be constructed from metric fluctuations of the form

$$h_{\mu\nu} = \mathcal{L}_\xi \bar{g}_{\mu\nu} \,, \tag{4.4.2}$$

subject to the conditions of normalizability,

$$(h_{\mu\nu}, h_{\mu\nu}) = 1 \,, \tag{4.4.3}$$

transversality,

$$\bar{\nabla}^\mu h_{\mu\nu} = 0 \,, \tag{4.4.4}$$

and tracelessness,

$$\bar{g}^{\mu\nu} h_{\mu\nu} = 0 \,. \tag{4.4.5}$$

A key feature of these modes is that they are generated by vector fields ξ^μ which are non-normalizable. As a consequence, the associated diffeomorphisms act non-trivially on the asymptotic region of the near-horizon extremal geometry, thereby giving rise to physical zero modes (see, for instance, [38]).

The spectrum of zero modes of the operator $\mathbb{O}_{\mathrm{AdS}_2\times S^3}$ can be organized into distinct families, each contributing to the logarithmic corrections under consideration. In particular, one finds two classes of gravitational zero modes, together with additional contributions arising from the $U(1)$ gauge sector.

In the following, we analyze each family of modes separately, beginning with the gravitational sector and subsequently turning to the gauge-field contributions.

4.4.1 Tensor Modes

The tensor zero modes are constructed from scalar functions on the AdS_2 factor. More precisely, they arise from solutions of the equation

$$\left(\bar{\Box}_{\mathrm{AdS}_2} + R_{\mathrm{AdS}_2}\right) B(\tau,\eta) = 0\,, \tag{4.4.6}$$

where $\bar{\Box}_{\mathrm{AdS}_2}$ and R_{AdS_2} denote the Laplacian and Ricci scalar associated with the AdS_2 metric (3.3.5).

Given a solution B, the corresponding metric perturbation is generated by a diffeomorphism,

$$h_{\mu\nu} = \mathcal{L}_\xi \bar{g}_{\mu\nu}\,, \qquad \xi = \bar{g}^{\mu\nu}\xi^\flat_\mu \partial_\nu\,, \qquad \xi^\flat = \star_{\mathrm{AdS}_2} dB\,, \tag{4.4.7}$$

where $\star_{\mathrm{AdS}_2}$ denotes the Hodge dual with respect to the AdS_2 metric.

This construction follows from the traceless condition $\bar{g}^{\mu\nu}h_{\mu\nu} = 0$, which implies $d\star_{\mathrm{AdS}_2}\xi^\flat = 0$. By Poincaré's lemma, this condition is locally solved by $\xi^\flat = \star_{\mathrm{AdS}_2} dB$ for some scalar function B. The transversality condition $\bar{\nabla}^\mu h_{\mu\nu} = 0$ then leads precisely to (4.4.6).

For the background under consideration, the normalized tensor perturbations take the explicit form

$$h^{(n)}_{\mu\nu} dx^\mu dx^\nu = \frac{\mathrm{i}\, e^{in\tau}\, \ell_{\mathrm{AdS}} \sqrt{|n|(n^2-1)}}{2\pi^{3/2} r_0^{3/2}} \tanh^{|n|}\!\left(\frac{\eta}{2}\right) \left(\mathrm{i}\, d\tau + \frac{d\eta}{\sinh\eta}\right)^2\,, \tag{4.4.8}$$

with $|n| = 2, 3, \ldots$, where normalizability on the extremal near-horizon geometry excludes the lowest modes.

At finite but small temperature, these zero modes are lifted. The corresponding first-order correction to the eigenvalues is given by

$$\begin{aligned} \delta\lambda_n^{\text{tensor}} &= \left(h^{(n)}_{\mu\nu}, \delta\mathbb{O}\, h^{(n)}_{\mu\nu}\right) = \int d^5x \sqrt{\bar{g}}\, h^{(n)*}_{\mu\nu}\, \delta\mathsf{D}^{\mu\nu,\rho\sigma} h^{(n)}_{\rho\sigma}\,, \\ &= \frac{|n|\,T}{T_{\text{tensor}}} + \mathcal{O}(T^2)\,, \end{aligned} \tag{4.4.9}$$

where the characteristic scale is

$$T_{\text{tensor}} = \frac{64Gr_0^3}{3\pi\,(4\alpha + r_0^2)}\,. \tag{4.4.10}$$

As in General Relativity, the lifting of the zero modes is linear in the mode number n. This behavior leads to the well-known $3/2$ coefficient in the logarithmic correction to the entropy of extremal black holes at small temperature and fixed charge.

Finally, it is worth emphasizing that for positive Gauss-Bonnet coupling α, as suggested by string theory, the scale T_{tensor} is manifestly positive. Moreover, for fixed horizon radius r_0, the correction depends linearly on α, reflecting the perturbative role of the higher-curvature interaction in the spectrum of fluctuations.

4.4.2 Vector Modes

The vector modes are constructed by combining scalar functions on AdS_2 with Killing one-forms on the three-sphere. More precisely, they are generated from solutions of

$$\bar{\Box}_{\text{AdS}_2} V(\tau, \eta) = 0\,, \tag{4.4.11}$$

which provide the AdS_2 dependence of the perturbation.

Given such a solution V_n, the corresponding metric fluctuation is defined as

$$h_{\mu\nu}^{(n,m)} dx^\mu dx^\nu = dV_n \otimes \zeta_m + \zeta_m \otimes dV_n = 2\,\zeta_{(m} dV_{n)}\,, \tag{4.4.12}$$

where n labels the eigenmodes of (4.4.11), and ζ_m denotes a basis of one-forms on S^3 whose dual vector fields generate the isometries of the sphere.

For the metric (3.3.6), the isometry algebra is $\mathfrak{so}(4) \cong \mathfrak{su}(2) \oplus \mathfrak{su}(2)$. A convenient complex basis is given by

$$\zeta_1 = e^{\mathrm{i}\phi}(d\theta - \mathrm{i}\sin\theta d\psi)\,, \qquad \zeta_4 = e^{\mathrm{i}\psi}(d\theta - \mathrm{i}\sin\theta d\phi)\,, \tag{4.4.13}$$

$$\zeta_2 = e^{-\mathrm{i}\phi}(d\theta + \mathrm{i}\sin\theta d\psi)\,, \qquad \zeta_5 = e^{-\mathrm{i}\psi}(d\theta + \mathrm{i}\sin\theta d\phi)\,, \tag{4.4.14}$$

$$\zeta_3 = \mathrm{i}\sqrt{2}(d\phi + \cos\theta d\psi)\,, \qquad \zeta_6 = \mathrm{i}\sqrt{2}(d\psi + \cos\theta d\phi)\,, \tag{4.4.15}$$

where ζ_3 and ζ_6 generate the Cartan subalgebra. These one-forms satisfy the

Maurer Cartan relations, for instance

$$\sqrt{2}\, d\zeta_1 + \zeta_1 \wedge \zeta_3 = 0\,, \tag{4.4.16}$$

with analogous relations for the remaining generators.

Regularity of $V(\tau, \eta)$ at the origin implies that the general solution to (4.4.11) is

$$V_n(\tau, \eta) = A_n\, e^{in\tau}\, \tanh^{|n|}\left(\frac{\eta}{2}\right)\,, \tag{4.4.17}$$

where A_n is a normalization constant. The corresponding normalized perturbation is

$$h^{(m,n)} = \frac{1}{8\sqrt{\pi^3 |n| r_0}} e^{in\tau}\, \tanh^{|n|}\left(\frac{\eta}{2}\right) \left(in d\tau + \frac{|n|}{\cosh\eta} d\eta\right) \otimes_s \zeta_m\,, \tag{4.4.18}$$

where $\otimes_s$ denotes the symmetric tensor product without the conventional factor of $1/2$.

The lifting of these zero modes at finite temperature is determined by

$$\begin{aligned} \delta\lambda_{m,n}^{\text{vector}} &= \left(h^{(m,n)}, \delta\mathbb{O}\, h^{(m,n)}\right) = \int d^5x \sqrt{g}\, h_{\mu\nu}^{(m,n)*}\, \delta\mathsf{D}^{\mu\nu,\rho\sigma} h_{\rho\sigma}^{(m,n)} \\ &= \frac{|n|\, T}{T_{\text{vector}}} + \mathcal{O}(T^2)\,, \end{aligned} \tag{4.4.19}$$

with

$$T_{\text{vector}} = \frac{48 G r_0^3 (4\alpha + r_0^2)(\Lambda r_0^2 - 2)}{\pi\left(-48\alpha^2 + 24\alpha^2 \Lambda r_0^2 + 4\alpha\Lambda r_0^4 - 12\alpha r_0^2 + \Lambda r_0^6 - 3r_0^4\right)}\,. \tag{4.4.20}$$

In this case, $|n| = 1, 2, \ldots$, as required by normalizability. The correction is independent of the index m, reflecting the degeneracy associated with the S^3 isometries.

The sign of the correction depends sensitively on the Gauss Bonnet coupling. For $\alpha > -r_0^2/4$, one finds $\delta\lambda_{m,n}^{\text{vector}} > 0$ for any $\Lambda < 0$, whereas for $\alpha < -r_0^2/4$ the correction becomes negative.

Expanding for small Gauss Bonnet coupling, one obtains

$$\delta\lambda^{\text{vector}}_{m,n} = \frac{|n|\pi T}{G r_0^3}\left[\frac{r_0^2(3-r_0^2\Lambda)}{2-r_0^2\Lambda} + \frac{\alpha^2}{2r_0^2} - \frac{2\alpha^3}{r_0^4} + \mathcal{O}\left(\frac{\alpha^4}{r_0^6}\right)\right]. \tag{4.4.21}$$

Interestingly, the linear correction in α is absent, indicating that the leading Gauss Bonnet effect in this sector arises only at quadratic order.

4.4.3 $U(1)$ gauge modes

The $U(1)$ gauge modes $a_\mu(x)$ arise as zero-modes of the operator (4.3.23) and are required to satisfy the gauge-fixing condition $\bar{\nabla}_\mu a^\mu = 0$. Pure gauge configurations, namely $a_\mu = \partial_\mu V$, automatically lie in the kernel of (4.3.23). The gauge condition then implies that the scalar function V must satisfy $\bar{\Box} V = 0$.

Exploiting the direct product structure of the background geometry, the relevant solutions are those with non-trivial dependence along AdS_2, which coincide with the solutions of (4.4.11). These modes are therefore labeled by an integer n and take the form

$$a^{(n)}_\mu dx^\mu = \frac{1}{2\sqrt{|n|\pi^3 r_0^3}} e^{in\tau} \tanh^{|n|}\left(\frac{\eta}{2}\right)\left(in\, d\tau + \frac{|n|}{\sinh\eta} d\eta\right). \tag{4.4.22}$$

Normalizability requires $|n| = 1, 2, \ldots$, and these modes form an orthonormal set with respect to the inner product, $(a^{(n)}, a^{(m)}) = \delta_{n,m}$.

The leading temperature correction to these $U(1)$ zero-modes is given by

$$\begin{aligned}\delta\lambda^{U(1)}_n = \left(a^{(n)}_\mu, \delta\mathbb{O} a^{(n)}_\mu\right) &= \int d^5x \sqrt{\bar{g}}\, a^*_\mu\, \delta \mathsf{D}^{\mu,\rho} a_\rho \\ &= \frac{|n| T}{T_{U(1)}} + \mathcal{O}(T^2)\,,\end{aligned} \tag{4.4.23}$$

with

$$T_{U(1)} = -\frac{12 G r_0 \,(4\alpha + r_0^2)\,(\Lambda r_0^2 - 2)}{\pi\,(-24\alpha + 16\alpha\Lambda r_0^2 + \Lambda r_0^4)}\,. \tag{4.4.24}$$

This correction is non-vanishing only when either α or Λ is different from zero. For $\Lambda < 0$ and $\alpha > 0$, it is always negative, in agreement with the behavior already observed in General Relativity with a negative cosmological constant, where the contribution vanishes in the limit $\Lambda \to 0$ (see, e.g., Eq. (4.31) of [41]). Allowing

$\Lambda > 0$, one finds parameter regions where the correction becomes positive.

For small Gauss Bonnet coupling, $\alpha/r_0^2 \ll 1$, the expansion reads

$$\delta\lambda_n^{U(1)} = \frac{\pi|n|T}{Gr_0}\left[-\frac{\Lambda r_0^2}{12\,(\Lambda r_0^2-2)} - \frac{\alpha}{r_0^2} + \frac{4\alpha^2}{r_0^4} - \frac{16\alpha^3}{r_0^6} + \mathcal{O}\left(\frac{\alpha^4}{r_0^6}\right)\right]. \tag{4.4.25}$$

It is worth emphasizing that these $U(1)$ gauge zero-modes are also annihilated by the interaction operator (4.3.22). Consequently, obtaining a non-vanishing interaction contribution requires considering perturbations that are not generated by a pure gauge transformation.

Possible existence of additional modes. In three dimensions, there exist non-trivial tensor modes that are eigenfunctions of the Laplace Beltrami operator. Since the near-horizon geometry contains a three-sphere, it is natural to investigate whether analogous tensorial perturbations on S^3 could contribute to the path integral.

Consider a maximally symmetric p-dimensional manifold N with metric γ_{ij}, curvature K, and covariant derivative D_i. Let us restrict to perturbations generated by a gauge transformation, $h_{ij} = 2D_{(i}\xi_{j)}$, which are required to be traceless, $\gamma^{ij}h_{ij} = 0$, and transverse, $D_ih^{ij} = 0$. These conditions imply

$$D_iD^i\xi^j = -K(p-1)\,\xi^j\,, \tag{4.4.26}$$

so that ξ^j must be a vector harmonic on N.

For $N = S^p$, the spectrum of vector harmonics is known, and the eigenvalue condition reduces to

$$p = l(l+p-1)\,, \qquad l = 1, 2, \ldots \tag{4.4.27}$$

which admits only the solution $l = 1$. This corresponds to the $p(p+1)/2$ Killing vectors of the sphere, for which the associated perturbation h_{ij} vanishes identically. Therefore, no additional transverse-traceless tensor modes generated by gauge transformations contribute in this sector. With support along the sphere.

Taking all contributions into account, we are finally in a position to assemble the one loop answer. The tensor modes (4.4.8), gravitational vector modes (4.4.18), and $U(1)$ gauge modes (4.4.22) each contribute an infinite tower of lifted zero modes, and their combined effect on the one loop partition function is obtained using zeta-function regularization. A detailed derivation of these regularized infinite products can be found, for example, in Kirsten's textbook [44]:

$$\prod_{n=2}^{\infty} \frac{\xi}{n} = \frac{1}{\xi^{3/2}\sqrt{2\pi}}\,, \qquad \prod_{n=1}^{\infty} \frac{\xi}{n} = \frac{1}{\sqrt{2\pi\xi}}\,. \tag{4.4.28}$$

Accounting for the contributions from positive and negative mode numbers, one finds

$$\log Z^{(0)}_{\text{1-loop}} = \frac{3}{2}\log\frac{T}{T_{\text{tensor}}} + \frac{6}{2}\log\frac{T}{T_{\text{vector}}} + \frac{1}{2}\log\frac{T}{T_{U(1)}} + \dots\,, \tag{4.4.29}$$

where the ellipsis denotes temperature-independent constants. The factor of 6 in the vector contribution arises from the six independent Killing vectors of S^3, each generating a tower of modes contributing a factor of $1/2$. This formula is the practical payoff of the whole operator analysis: once the near-extremal lifting of the zero modes is known, the logarithmic temperature dependence follows directly.

4.4.4 Entropy correction and the near-extremal density of states

Eq. (4.4.29) allows one to read off the leading one loop contribution to the thermodynamics in the canonical ensemble. Summing the three sectors, the temperature-dependent part of the one loop partition function is

$$\log Z^{(0)}_{\text{1-loop}} = 5\log\left(\frac{T}{T_0}\right) + \mathcal{O}(T^0)\,. \tag{4.4.30}$$

Here T_0 is a reference temperature scale, and $\mathcal{O}(T^0)$ stands for temperature-independent constants, including the scales T_{tensor}, T_{vector}, and $T_{U(1)}$, which do not affect the logarithmic dependence of the entropy. A natural choice, obtained by combining the three sectors in Eq. (4.4.29), is

$$T_0^5 = T_{\text{tensor}}^{3/2} T_{\text{vector}}^{3} T_{U(1)}^{1/2}, \qquad T_0 = \left(T_{\text{tensor}}^{3/2} T_{\text{vector}}^{3} T_{U(1)}^{1/2}\right)^{1/5}. \tag{4.4.31}$$

This choice is not universal: changing T_0 only shifts $\log Z^{(0)}_{\text{1-loop}}$ by a temperature-independent constant and therefore leaves the logarithmic coefficient equal to 5.

At fixed charge, the entropy is obtained from the canonical relation

$$S(T,Q) = \left(1 - \beta\frac{\partial}{\partial\beta}\right)\log Z(\beta,Q) \qquad \text{with} \qquad \beta = T^{-1}\,. \tag{4.4.32}$$

Applying this formula to the one loop contribution (4.4.30), one finds

$$\Delta S_{\text{1-loop}}(T,Q) = 5\log\left(\frac{T}{T_0}\right) + \mathcal{O}(T^0)\,. \tag{4.4.33}$$

Therefore, the logarithmic correction anticipated on general grounds in Chapter 3 is realized explicitly in the present Einstein Gauss Bonnet Maxwell background, with overall coefficient equal to 5.

Combining this result with the classical near-extremal thermodynamics discussed in the previous chapter, the entropy at small temperature and fixed charge takes the form

$$S(T,Q) \approx S_{\text{ext}}(Q) + \frac{2T}{M_{\text{gap}}} + 5\log\left(\frac{T}{T_0}\right). \tag{4.4.34}$$

Using the first law in the canonical ensemble, $dE = T\,dS$ with $E := M - M_{\text{ext}}$, we then obtain

$$\frac{dE}{dT} = T\frac{dS}{dT} = \frac{2T}{M_{\text{gap}}} + 5 + \mathcal{O}(T) \tag{4.4.35}$$

and therefore

$$E(T) = 5T + \frac{T^2}{M_{\text{gap}}} + \mathcal{O}(T^2)\,. \tag{4.4.36}$$

This is the key physical effect of the one loop correction: the strict quadratic behavior of the classical near-extremal energy is replaced by a leading term linear in the temperature. As a consequence, the black hole now carries enough energy to emit arbitrarily soft Hawking quanta, and the classical mass-gap obstruction is softened.

The corresponding modification of the density of states can be inferred from the microcanonical relation

$$\rho(E) \sim e^{S(E)}\,. \tag{4.4.37}$$

In the very low-energy regime, Eq. (4.4.36) gives $T \simeq E/5$, so Eq. (4.4.34) becomes

$$S(E) \approx S_{\mathrm{ext}}(Q) + 5\log\left(\frac{E}{E_0}\right) + \frac{2E}{5M_{\mathrm{gap}}}\,. \tag{4.4.38}$$

where E_0 is a reference energy scale, and up to an additive constant that depends on the precise normalization of the one loop partition function. Exponentiating, one finds the qualitative near-extremal behavior

$$\rho(E) \propto e^{S_{\mathrm{ext}}}\left(\frac{E}{E_0}\right)^5 e^{\frac{2E}{5M_{\mathrm{gap}}}}\left[1 + \mathcal{O}(E)\right]. \tag{4.4.39}$$

This shows how the quantum effects modify the schematic profile displayed in Fig. 1.0.1 of the Introduction. Classically, the extremal state appears as a macroscopically degenerate ground state. After including the one-loop correction, the low-energy density of states acquires a power-law suppression controlled by the logarithmic term. In particular, the factor $(E/E_0)^5$ drives the effective density of states to zero as the extremal limit is approached. Thus, within the semiclassical approximation considered here, the apparent ground-state degeneracy is explicitly suppressed by the quantum correction.

Chapter 5

Conclusiones

En este trabajo se estudió el papel de las correcciones cuánticas de un loop en la termodinámica de agujeros negros cargados cercanos a la extremalidad en gravedad de Einstein-Gauss-Bonnet acoplada a un campo de Maxwell. El objetivo principal fue entender cómo las modificaciones de curvatura superior afectan el operador de fluctuaciones alrededor de la geometría de garganta y cómo, a través de sus modos cero, dichas fluctuaciones se reflejan en correcciones logarítmicas a la entropía.

El análisis comenzó con la formulación de la función de partición euclídea y su expansión semiclásica. Este marco permitió identificar de manera sistemática cómo las correcciones cuánticas de un loop se codifican en determinantes funcionales del operador cuadrático de fluctuaciones, y por qué los modos cero requieren un tratamiento separado en el régimen cercano a la extremalidad.

Posteriormente se revisó la solución cargada de Einstein-Maxwell-Gauss-Bonnet y su límite extremal. La presencia del término de Gauss-Bonnet modifica tanto la geometría como la entropía clásica de Wald, y en el régimen extremal la región cercana al horizonte desarrolla una garganta de tipo $AdS_2 \times S^3$. Esta geometría constituye el fondo natural sobre el cual se estudian las fluctuaciones cuánticas relevantes para la corrección de un loop.

En particular, las cantidades termodinámicas clásicas que organizan directamente el análisis son la masa y la entropía de Wald. Con las convenciones usadas en este trabajo,

$$M = \frac{3\pi m}{64G}, \qquad S = \frac{\pi^2 r_+^3}{2G}\left(1 + \frac{12\alpha}{r_+^2}\right). \tag{5.0.1}$$

Y la capacidad calorífica a carga fija viene dada por

$$C_q = \frac{3\pi^2 r_+ (r_+^2 + 4\alpha)^2 \left(3r_+^4 - \Lambda r_+^6 - 2q^2\right)}{2G\left(-\Lambda r_+^8 - 12\alpha\Lambda r_+^6 - 3r_+^6 + 12\alpha r_+^4 + 10q^2 r_+^2 + 24\alpha q^2\right)}. \tag{5.0.2}$$

Las expresiones para M y S resumen la termodinámica clásica sobre la cual se incorporan posteriormente las correcciones cuánticas.

El resultado central de este trabajo es que los modos cero del operador de fluctuaciones son levantados al considerar una temperatura pequeña pero finita. Este levantamiento produce una contribución logarítmica a la entropía,

$$\Delta S_{\text{1-loop}}(T,Q) = 5\log\left(\frac{T}{T_0}\right) + \mathcal{O}(T^0), \tag{5.0.3}$$

y por lo tanto la entropía corregida a baja temperatura contiene el término $5\log(T/T_0)$, donde T_0 es una escala de referencia con dimensiones de temperatura. Para temperaturas suficientemente bajas, esta contribución se vuelve grande y negativa, dominando el comportamiento hacia el límite extremal. En consecuencia, la degeneración macroscópica del estado fundamental sugerida por la entropía clásica no permanece intacta: al incluir la corrección de un loop, el número efectivo de estados asociados al límite de energía cero se anula. De manera equivalente, usando $\rho(E) \sim e^{S(E)}$, la corrección encontrada implica un comportamiento de la forma

$$\rho(E) \propto e^{S_{\text{ext}}}\left(\frac{E}{E_0}\right)^5 \tag{5.0.4}$$

donde E_0 es una escala de referencia con dimensiones de energía. Así, para energías suficientemente pequeñas, la densidad de estados queda suprimida y se aproxima a cero hacia el límite extremal.

Así, la corrección logarítmica proporciona una resolución clara, dentro del régimen semiclásico considerado, de la aparente gran degeneración del estado fundamental extremal: la contribución cuántica suprime explícitamente dicha degeneración en el límite de temperatura cero. Este resultado muestra que los términos sublíderes en la función de partición no son meras correcciones pequeñas al área, sino que pueden cambiar cualitativamente la interpretación microscópica del estado extremal.

Como posible dirección futura, sería natural extender este análisis a teorías de gravedad de orden superior más generales, como las teorías de Lovelock y las teorías quasitopológicas. Estas extensiones permitirían estudiar si la supresión de la degeneración del estado fundamental encontrada aquí persiste en familias más amplias de acciones efectivas y cómo depende de la estructura particular de los términos de curvatura superior. Además, un artículo reciente subido a arXiv [45] señala que, para ciertas contribuciones provenientes de modos vectoriales, el análisis realizado directamente en la geometría de horizonte cercano no es necesariamente equivalente al análisis que mantiene la geometría completa del agujero negro. Dado que este es un desarrollo reciente, sería interesante estudiar con mayor detalle si esas afirmaciones son compatibles con el caso considerado en esta tesis, o si la inclusión de la geometría completa modifica de manera no trivial la contribución de los modos vectoriales a la corrección logarítmica.

Conclusions

In this work we studied the role of one-loop quantum corrections in the thermodynamics of near-extremal charged black holes in Einstein-Gauss-Bonnet gravity coupled to a Maxwell field. The main goal was to understand how higher-curvature interactions modify the fluctuation operator around the near-horizon throat and how, through its zero modes, these fluctuations produce logarithmic corrections to the entropy.

The analysis began with the Euclidean partition function and its semiclassical expansion. This framework made it possible to identify systematically how one-loop quantum corrections are encoded in functional determinants of the quadratic fluctuation operator, and why zero modes require a separate treatment in the near-extremal regime.

We then reviewed the charged Einstein-Maxwell-Gauss-Bonnet solution and its extremal limit. The Gauss-Bonnet term modifies both the geometry and the classical Wald entropy, while the extremal near-horizon region develops an $AdS_2 \times S^3$ throat. This geometry provides the natural background on which the quantum fluctuations relevant for the one-loop correction are analyzed.

In particular, the classical thermodynamic quantities that directly organize the analysis are the mass and the Wald entropy. With the conventions used in this work,

$$M = \frac{3\pi m}{64G}, \qquad S = \frac{\pi^2 r_+^3}{2G}\left(1 + \frac{12\alpha}{r_+^2}\right). \tag{5.0.5}$$

And the heat capacity at fixed charge is

$$C_q = \frac{3\pi^2 r_+(r_+^2 + 4\alpha)^2 \left(3r_+^4 - \Lambda r_+^6 - 2q^2\right)}{2G\left(-\Lambda r_+^8 - 12\alpha\Lambda r_+^6 - 3r_+^6 + 12\alpha r_+^4 + 10q^2 r_+^2 + 24\alpha q^2\right)}. \tag{5.0.6}$$

The expressions for M and S summarize the classical thermodynamic background on top of which the quantum corrections are subsequently incorporated.

The central result of this thesis is that the zero modes of the fluctuation operator are lifted when a small but finite temperature is introduced. This lifting generates a logarithmic contribution to the entropy,

$$\Delta S_{\text{1-loop}}(T, Q) = 5\log\left(\frac{T}{T_0}\right) + \mathcal{O}(T^0), \tag{5.0.7}$$

so that the corrected low-temperature entropy contains the term $5\log(T/T_0)$, where T_0 is a reference scale with dimensions of temperature. At sufficiently low temperatures, this contribution becomes large and negative, controlling the behavior toward the extremal limit. Therefore, the macroscopic ground-state degeneracy suggested by the classical entropy is not preserved: once the one-loop correction is included, the effective number of states associated with the zero-energy limit vanishes. Equivalently, using $\rho(E) \sim e^{S(E)}$, the correction implies the low-energy behavior

$$\rho(E) \propto e^{S_{\text{ext}}}\left(\frac{E}{E_0}\right)^5, \tag{5.0.8}$$

where E_0 is a reference scale with dimensions of energy. Thus, at sufficiently low energies, the density of states is suppressed and approaches zero toward the extremal limit.

Thus, the logarithmic correction gives a direct semiclassical mechanism by which the apparent large degeneracy of the extremal ground state is explicitly suppressed. This shows that subleading terms in the partition function are not only quantitative corrections to the area contribution, but can qualitatively change the microscopic interpretation of the extremal state.

As a possible future direction, it would be natural to extend this analysis to more general higher-curvature theories, such as Lovelock gravity and quasitopological gravity. These extensions would make it possible to test whether the suppression of the ground-state degeneracy found here persists in broader families of effective gravitational actions, and how it depends on the specific structure of the higher-curvature terms. In addition, a recent arXiv article [45] points out that, for certain contributions arising from vector modes, the computation performed directly in the near-horizon geometry is not necessarily equivalent to the computation that keeps the full black hole geometry. Since this is a recent development, it would be interesting to examine in detail whether those statements are compatible with the case studied in this thesis, or whether the inclusion of the full geometry modifies the vector-mode contribution to the logarithmic correction in a non-trivial way.

Bibliography

[1] B. P. Abbott et al. Binary Black Hole Mergers in the first Advanced LIGO Observing Run. *Phys. Rev. X*, 6(4):041015, 2016. doi: 10.1103/PhysRevX.6.041015. [Erratum: Phys.Rev.X 8, 039903 (2018)].

[2] Jacob D. Bekenstein. Black holes and entropy. *Phys. Rev. D*, 7:2333–2346, 1973. doi: 10.1103/PhysRevD.7.2333.

[3] S. W. Hawking. Particle creation by black holes. *Commun. Math. Phys.*, 43: 199, 1975.

[4] Juan Maldacena. The large-n limit of superconformal field theories and supergravity. *International Journal of Theoretical Physics*, 38(4):1113–1133, April 1999. ISSN 1572-9575. doi: 10.1023/a:1026654312961. URL http://dx.doi.org/10.1023/A:1026654312961.

[5] Edward Witten. Anti de sitter space and holography, 1998. URL https://arxiv.org/abs/hep-th/9802150.

[6] John Preskill, Patricia Schwarz, Alfred D. Shapere, Sandip Trivedi, and Frank Wilczek. Limitations on the statistical description of black holes. *Mod. Phys. Lett. A*, 6:2353–2362, 1991. doi: 10.1142/S0217732391002773.

[7] Juan Martin Maldacena, Jeremy Michelson, and Andrew Strominger. Anti-de Sitter fragmentation. *JHEP*, 02:011, 1999. doi: 10.1088/1126-6708/1999/02/011.

[8] Don N. Page. Thermodynamics of near extreme black holes. In *Proceedings of the 9th Marcel Grossmann Meeting*, 9 2000.

[9] Ahmed Almheiri, Thomas Hartman, Juan Maldacena, Edgar Shaghoulian, and Amirhossein Tajdini. The entropy of Hawking radiation. *Rev. Mod. Phys.*, 93(3):035002, 2021. doi: 10.1103/RevModPhys.93.035002.

[10] Andrew Strominger and Cumrun Vafa. Microscopic origin of the Bekenstein-Hawking entropy. *Phys. Lett. B*, 379:99–104, 1996. doi: 10.1016/0370-2693(96)00345-0.

[11] K. S. Stelle. Renormalization of higher derivative quantum gravity. *Phys. Rev. D*, 16:953, 1977.

[12] D. Lovelock. The Einstein tensor and its generalizations. *J. Math. Phys.*, 12: 498–501, 1971. doi: 10.1063/1.1665613.

[13] B. Zwiebach. Curvature squared terms and string theories. *Phys. Lett. B*, 156:315, 1985.

[14] R. R. Metsaev and Arkady A. Tseytlin. Order alpha-prime (Two Loop) Equivalence of the String Equations of Motion and the Sigma Model Weyl Invariance Conditions: Dependence on the Dilaton and the Antisymmetric Tensor. *Nucl. Phys. B*, 293:385–419, 1987. doi: 10.1016/0550-3213(87) 90077-0.

[15] Pablo A. Cano and Alejandro Ruipérez. String gravity in D=4. *Phys. Rev. D*, 105(4):044022, 2022. doi: 10.1103/PhysRevD.105.044022.

[16] Yves Brihaye, Burkhard Kleihaus, Jutta Kunz, and Eugen Radu. Rotating black holes with equal-magnitude angular momenta in d = 5 einstein-gauss-bonnet theory. *Journal of High Energy Physics*, 2010(11), November 2010. ISSN 1029-8479. doi: 10.1007/jhep11(2010)098. URL http://dx.doi.org/10.1007/JHEP11(2010)098.

[17] Sergei N. Solodukhin. The Conical singularity and quantum corrections to entropy of black hole. *Phys. Rev. D*, 51:609–617, 1995. doi: 10.1103/PhysRevD.51.609.

[18] Dmitri V. Fursaev. Temperature and entropy of a quantum black hole and conformal anomaly. *Phys. Rev. D*, 51:5352–5355, 1995. doi: 10.1103/PhysRevD.51.R5352.

[19] Ashoke Sen. Logarithmic Corrections to Schwarzschild and Other Non-extremal Black Hole Entropy in Different Dimensions. *JHEP*, 04:156, 2013. doi: 10.1007/JHEP04(2013)156.

[20] Shamik Banerjee, Rajesh K. Gupta, and Ashoke Sen. Logarithmic corrections to extremal black hole entropy from quantum entropy function. *Journal of High Energy Physics*, 2011(3), March 2011. ISSN 1029-8479. doi: 10.1007/jhep03(2011)147. URL http://dx.doi.org/10.1007/JHEP03(2011)147.

[21] Cynthia Keeler, Finn Larsen, and Pedro Lisbao. Logarithmic Corrections to $N \geq 2$ Black Hole Entropy. *Phys. Rev. D*, 90(4):043011, 2014. doi: 10.1103/PhysRevD.90.043011.

[22] Alejandra Castro, Victor Godet, Finn Larsen, and Yangwenxiao Zeng. Logarithmic Corrections to Black Hole Entropy: the Non-BPS Branch. *JHEP*, 05:079, 2018. doi: 10.1007/JHEP05(2018)079.

[23] Ashoke Sen. Logarithmic Corrections to Rotating Extremal Black Hole Entropy in Four and Five Dimensions. *Gen. Rel. Grav.*, 44:1947–1991, 2012. doi: 10.1007/s10714-012-1373-0.

[24] G. W. Gibbons and S. W. Hawking. Action Integrals and Partition Functions

in Quantum Gravity. *Phys. Rev. D*, 15:2752–2756, 1977. doi: 10.1103/PhysRevD.15.2752.

[25] Ashoke Sen. Quantum Entropy Function from AdS(2)/CFT(1) Correspondence. *Int. J. Mod. Phys. A*, 24:4225–4244, 2009. doi: 10.1142/S0217751X09045893.

[26] M. Nakahara. *Geometry, topology and physics*. Taylor & Francis, 2003.

[27] Robert C. Myers. Higher Derivative Gravity, Surface Terms and String Theory. *Phys. Rev. D*, 36:392, 1987. doi: 10.1103/PhysRevD.36.392.

[28] Roberto Emparan, Clifford V. Johnson, and Robert C. Myers. Surface terms as counterterms in the AdS / CFT correspondence. *Phys. Rev. D*, 60:104001, 1999. doi: 10.1103/PhysRevD.60.104001.

[29] Yves Brihaye and Eugen Radu. Black objects in the Einstein-Gauss-Bonnet theory with negative cosmological constant and the boundary counterterm method. *JHEP*, 09:006, 2008. doi: 10.1088/1126-6708/2008/09/006.

[30] Giorgos Anastasiou, Ignacio J. Araya, Avik Chakraborty, Cristóbal Corral, and Rodrigo Olea. Renormalization of Einstein-Gauss-Bonnet AdS gravity. *JHEP*, 02:091, 2026. doi: 10.1007/JHEP02(2026)091.

[31] S. W. Hawking and Simon F. Ross. Duality between electric and magnetic black holes. *Phys. Rev. D*, 52:5865–5876, 1995. doi: 10.1103/PhysRevD.52.5865.

[32] Robert M. Wald. Black hole entropy is the Noether charge. *Phys. Rev. D*, 48 (8):R3427–R3431, 1993. doi: 10.1103/PhysRevD.48.R3427.

[33] Vivek Iyer and Robert M. Wald. Some properties of Noether charge and a proposal for dynamical black hole entropy. *Phys. Rev. D*, 50:846–864, 1994. doi: 10.1103/PhysRevD.50.846.

[34] Luca V. Iliesiu, Sameer Murthy, and Gustavo J. Turiaci. Revisiting the logarithmic corrections to the black hole entropy. *JHEP*, 07:058, 2025. doi: 10.1007/JHEP07(2025)058.

[35] Sudip Karan and Gurmeet Singh Punia. Logarithmic correction to black hole entropy in universal low-energy string theory models. *JHEP*, 03:028, 2023. doi: 10.1007/JHEP03(2023)028.

[36] Nabamita Banerjee and Muktajyoti Saha. Revisiting leading quantum corrections to near extremal black hole thermodynamics. *JHEP*, 07:010, 2023. doi: 10.1007/JHEP07(2023)010.

[37] Daniel Kapec, Ahmed Sheta, Andrew Strominger, and Chiara Toldo. Logarithmic Corrections to Kerr Thermodynamics. *Phys. Rev. Lett.*, 133(2): 021601, 2024. doi: 10.1103/PhysRevLett.133.021601.

[38] Ilija Rakic, Mukund Rangamani, and Gustavo J. Turiaci. Thermodynamics of the near-extremal Kerr spacetime. *JHEP*, 06:011, 2024. doi: 10.1007/JHEP06(2024)011.

[39] Sabyasachi Maulik, Leopoldo A. Pando Zayas, Augniva Ray, and Jingchao Zhang. Universality in logarithmic temperature corrections to near-extremal rotating black hole thermodynamics in various dimensions. *JHEP*, 06:034, 2024. doi: 10.1007/JHEP06(2024)034.

[40] Sabyasachi Maulik, Arpita Mitra, Debangshu Mukherjee, and Augniva Ray. Logarithmic corrections to near-extremal entropy of charged de Sitter black holes. *JHEP*, 01:156, 2026. doi: 10.1007/JHEP01(2026)156.

[41] Matthew J. Blacker, Alejandra Castro, Watse Sybesma, and Chiara Toldo. Quantum corrections to the path integral of near extremal de Sitter black holes. *JHEP*, 08:120, 2025. doi: 10.1007/JHEP08(2025)120.

[42] Lucas Acito and Matías N. Sempé. From BTZ Perturbations to Schwarzian Modes: A Geometrical and Perturbative Analysis. *arXiv preprint*, 11 2025.

[43] Leopoldo A. Pando Zayas and Jingchao Zhang. A Universality Theorem for the Quantum Thermodynamics of Near-Extremal Black Holes. *arXiv preprint*, 2 2026.

[44] Klaus Kirsten. *Spectral Functions in Mathematics and Physics*. Chapman and Hall/CRC, Boca Raton, 2001.

[45] Adam Bac, Alejandra Castro, and Diksha Jain. Revisiting near-extremal and near-BPS black holes in AdS3 supergravity. *arXiv preprint*, 4 2026.

Appendix A

Embedding of AdS_2

A1 Geometry of AdS_2

Anti-de Sitter space can be defined as a hyperboloid embedded in a higher-dimensional flat space. In the case of AdS_2, this corresponds to the surface

$$\mathrm{AdS}_2 = \left\{(X_{-1}, X_0, X_1) \in \mathbb{R}^3 : -X_{-1}^2 + X_0^2 - X_1^2 = -\ell^2\right\}. \tag{A1.1}$$

Different coordinate systems can be introduced depending on how the hyperboloid is parametrized. A convenient choice is given by global coordinates, defined through

$$\begin{aligned} X_{-1} &= \ell \cosh\rho \cos T, \\ X_0 &= \ell \sinh\rho, \\ X_1 &= \ell \cosh\rho \sin T, \end{aligned} \tag{A1.2}$$

which lead to the metric

$$ds^2 = \ell^2 \left(-\cosh^2\rho\, dT^2 + d\rho^2\right). \tag{A1.3}$$

These coordinates cover the entire AdS_2 spacetime.

An alternative parametrization gives rise to a Rindler-like patch, with metric

$$ds^2 = \ell^2 \left(-\sinh^2\rho\, dT^2 + d\rho^2\right), \tag{A1.4}$$

which only covers a portion of the full manifold.

Another useful coordinate system is provided by the Poincaré patch, defined by

$$ds^2 = -\frac{r^2}{\ell^2}dt^2 + \frac{\ell^2}{r^2}dr^2. \tag{A1.5}$$

The relation between the Rindler-like and Poincaré patches can be obtained by comparing their embeddings in the ambient space. The corresponding transformation is

$$r = \ell(\cosh\rho - \cosh T \sinh\rho), \tag{A1.6}$$

$$t = \frac{\ell \sinh\rho \sinh T}{\cosh\rho - \cosh T \sinh\rho}. \tag{A1.7}$$

Applying this transformation to the near-horizon configuration obtained previously, one finds

$$ds^2 = \ell^2_{\mathrm{AdS}_2}\left(-\sinh^2\rho\, dT^2 + d\rho^2\right) + r_+^2 ds^2(S^3), \tag{A1.8}$$

$$F = \ell^2_{\mathrm{AdS}_2}\frac{\sqrt{3r_+^4 - r_+^6\Lambda}}{r_+^3}\sinh\rho\, d\rho \wedge dT. \tag{A1.9}$$

A corresponding gauge potential that reproduces this field strength is given by

$$A = \frac{\ell^2_{\mathrm{AdS}_2}}{r_+}\sqrt{3 - r_+^2\Lambda}\,(\cosh\rho - 1)\, dT. \tag{A1.10}$$

Appendix B

Expansion of r_+ and r_-

B.1 Expansion of r_+ and r_-

We aim to obtain an expansion of the horizon radii r_+ and r_- in powers of the temperature T in the canonical ensemble. This corresponds to keeping the charge Q fixed at its extremal value Q_0, which in turn implies that the charge parameter q is also fixed. In what follows, we present two methods to derive these expansions.

B.1.1 Method 1

Starting from the expression for the temperature,

$$T = \frac{f'(r_+)}{4\pi} = \frac{1}{24\alpha\pi r_+^5\sqrt{\Delta}}\left[r_+^6\left(3\sqrt{\Delta} - \sqrt{3}(4\alpha\Lambda + 3)\right) - 8\sqrt{3}\alpha q^2\right], \tag{B.1.1}$$

where

$$\Delta \equiv 3 + 4\alpha\Lambda + \frac{3\alpha m}{r_+^4} - \frac{16\alpha q^2}{r_+^6}, \tag{B.1.2}$$

one can solve for the mass parameter m as a function of r_+, T, and q, obtaining

$$\begin{aligned} m = \frac{1}{9r_+^6(r_+ - 8\pi\alpha T)^2} &\left[4(3 + 4\alpha\Lambda)(16\alpha q^4 + r_+^{10}(12\pi r_+ T - 48\pi^2\alpha T^2 + r_+^2\Lambda))\right. \\ &\left. + 8q^2 r_+^4(-24\pi\alpha r_+ T + 96\pi^2\alpha^2 T^2 + r_+^2(3 + 2\alpha\Lambda))\right]. \end{aligned} \tag{B.1.3}$$

Since α and Λ are constants, expressing $m = m(r_+, T, q)$ implicitly assumes that r_+ depends on the temperature. In particular, as the temperature is increased from $T = 0$, the horizon radius r_+ deviates from its extremal value r_0. Therefore, once the temperature T and charge parameter q are fixed, the mass parameter m is fully determined. Different black hole configurations correspond to different values of T while keeping q fixed.

In what follows, we choose this fixed value of the charge to be its extremal value, $q = q_{\text{ext}} = q_0$. From this point on, we will replace q by q_0.

From the expression for the charge in terms of r_+ and r_- (see (3.2.7)), in the extremal case where $r_+ = r_- = r_0$, the charge is given by

$$q_0^2 = \frac{r_0^4}{2}(r_0^2\Lambda - 3). \tag{B.1.4}$$

Substituting (B.1.4) into (B.1.3) and then into the metric function $f(r)$, we obtain an expression of the form $f = f(r_+, r_0, T)$:

$$f(r_+) = \frac{1}{12\alpha}\left(3r_+^2 + 12\alpha - r_+^2\sqrt{\frac{r_+^6(3+4\alpha\Lambda)^2 - 4\alpha r_0^4(r_0^2\Lambda - 3)}{r_+^{10}(r_+ - 8\pi T\alpha)^2}}\right). \tag{B.1.5}$$

We now assume the following ansatz for r_+ as a power series in T, up to order T^3:

$$r_+(T) = r_0 + d_1 T + d_2 T^2 + d_3 T^3. \tag{B.1.6}$$

Substituting this ansatz into (B.1.5), performing a Taylor expansion around $T = 0$, and imposing the condition $f(r_+) = \mathcal{O}(T^4)$ order by order, allows us to determine the coefficients d_1, d_2, and d_3.

A similar procedure can be applied to the inner horizon r_-. Substituting $q = q_0$ into $f(r_-)$ yields an expression analogous to (B.1.5), now depending on both r_+ and r_-. Using the expansion (B.1.6) together with the ansatz

$$r_-(T) = r_0 + z_1 T + z_2 T^2 + z_3 T^3, \tag{B.1.7}$$

and again expanding around $T = 0$ while imposing $f(r_-) = \mathcal{O}(T^4)$ order by order, one can solve for the coefficients z_1, z_2, and z_3.

B.1.2 Method 2

In this approach, we begin by assuming from the outset that both horizon radii r_+ and r_- admit expansions in powers of the temperature T:

$$r_+(T) = r_0 + d_1 T + d_2 T^2 + d_3 T^3, \tag{B.1.8}$$

$$r_-(T) = r_0 + z_1 T + z_2 T^2 + z_3 T^3. \tag{B.1.9}$$

Substituting these ansätze into the expression for the charge parameter $q = q(r_+, r_-)$ given in (3.2.7), and imposing that the charge remains fixed at its extremal value, one obtains constraints among the coefficients. More precisely, by expanding in powers of T and requiring that $q = q_0 + \mathcal{O}(T^4)$, one finds the relations

$$z_1 = -d_1, \tag{B.1.10}$$

$$z_2 = -d_2 + \frac{d_1^2(r_0^2\Lambda - 6)}{3r_0(r_0^2\Lambda - 2)}, \tag{B.1.11}$$

$$z_3 = -\frac{d_1^3(r_0^2\Lambda - 6)^2 + 9r_0^2 d_3(r_0^2\Lambda - 2)^2 - 6r_0 d_1 d_2(12 - 8r_0^2\Lambda + r_0^4\Lambda^2)}{9r_0^2(r_0^2\Lambda - 2)^2}. \tag{B.1.12}$$

Next, we substitute the expansions (B.1.8) and (B.1.9) into the temperature expression $T = T(r_+, r_-)$ given in (3.2.14). Using the relations (B.1.10) (B.1.12) to express z_1, z_2, and z_3 in terms of d_1, d_2, and d_3, we perform a Taylor expansion around $T = 0$ up to order T^4.

By solving the resulting equations order by order in T, one determines the coefficients d_1, d_2, and d_3. The coefficients z_1, z_2, and z_3 then follow directly by substituting these results back into (B.1.10), (B.1.11), and (B.1.12).